Electronic Supplementary Material (ESI) for ChemComm.

Supplementary Information

A macrocyclic 'Co^0' complex: the relevance of ligand non-innocence to reactivity

Manuel Kaspar[†], Philipp J. Altmann[†], Alexander Pöthig[†], Stephen Sproules[§], Corinna R. Hess[†]*

[†]Department of Chemistry and Catalysis Research Center, Technische Universität München (TUM), Lichtenbergstrasse 4, D-85747 Garching, Germany

[§]WestCHEM, School of Chemistry, University of Glasgow, Glasgow, G12 8QQ, United Kingdom

Table of Contents

Experimental

Materials and methods

Chemicals were purchased from Sigma Aldrich and used as received unless otherwise noted. Metal compounds were synthesized in an inert atmosphere glove box (argon), using anhydrous solvents. The solvents were dried by passage over activated alumina columns from MBraun, deoxygenated by four freeze-pump-thaw cycles and stored over 3 Å (MeCN) or 4 Å activated molecular sieves. Triethylamine was degassed by sparging with argon and stored over 3 Å molecular sieves. $[Co(CH_3CN)_6](PF_6)_2$ was synthesized according to the literature procedure for the synthesis of $[Co(CH_3CN)_6](BF_4)_2$, using $NO(PF_6)$ instead of $NO(BF_4)$ as the oxidant.[1] *p*-Cyanoanilinium tetrafluoroborate (*p*CA) was prepared as described in the literature.[2] Tetrabutylammonium hexafluorophosphate was recrystallized in EtOH four times before use. Ferrocene was sublimed before use. H(Mabiq) and Co(Mabiq) were synthesized as previously described.[3-5]

Solution state NMR spectra were measured on a Bruker Avance Ultrashield (400 MHz ^1H) spectrometer. X-band EPR spectra were recorded on a Bruker ELEXSYS E500 spectrometer or on a JEOL JES-FA 200 spectrometer, and simulations performed with Bruker's Xsophe software package.[6] Electronic spectra were measured on a Shimadzu UV-3600 Plus UV-vis-NIR spectrophotometer or an Agilent Cary 60 UV-vis spectrophotometer. ESI mass spectra were measured on a Thermo Scientific™ UltiMate™ 3000 HPLC System using the loop mode. Microanalyses were carried out at the Technische Universität München. Electrochemical measurements were carried out with an EmStat^{3+} potentiostat using a three-electrode cell equipped with glassy carbon working electrode, a Pt wire counter electrode and a $Ag/AgNO_3$ reference electrode. Potentials are reported with reference to an internal standard of ferrocenium/ferrocene ($Fc^{+/0}$).

Single crystal X-ray diffraction

General: For crystallization, pentane was allowed to diffuse slowly into a THF solution of compound **1**. Compound **2** was crystallized by slow evaporation of a concentrated Et_2O solution. Data were collected on an X-ray single crystal diffractometer equipped with a CMOS detector (Bruker Photon-100), a rotating anode (Bruker TXS) with MoK_α radiation ($\lambda = 0.71073$ Å) and a Helios mirror optic by using the APEX III software package.[7] The measurements were performed on a single crystal coated with perfluorinated ether. The crystal was fixed on top of a microsampler and transferred to the diffractometer. The crystal was frozen under a stream of cold nitrogen. A matrix scan was used to determine the initial lattice parameters. Reflections were merged and corrected for Lorentz and polarization effects, scan speed, and background using SAINT.[8] Absorption corrections, including odd and even ordered spherical harmonics, were performed using SADABS.[8] Space group assignments were based upon systematic absences, E statistics, and successful refinement of the structures. Structures were solved by direct methods with the aid of successive difference Fourier maps, and were refined against all data using SHELXLE[9] in conjunction with SHELXL-2014[10]. Hydrogen atoms were assigned to ideal positions and refined using a riding model with an isotropic thermal parameter 1.2 times that of the attached carbon atom (1.5 times for methyl hydrogen atoms). If not mentioned otherwise, non-hydrogen atoms were refined with anisotropic displacement parameters. Full-matrix least-squares refinements were carried out by minimizing $\Sigma w(Fo^2-Fc^2)^2$ with SHELXL-97[11] weighting scheme. Neutral atom scattering factors for all atoms and anomalous dispersion corrections for the non-hydrogen atoms were taken from International Tables for Crystallography.[12] Images of the crystal structures were generated by PLATON.[13-14]

Special:

[Co(Mabiq)(THF)](PF$_6$) (3): Geometrical restraints have been applied for disordered PF_6^- anions (see CIF).

[Co(Mabiq)Na(OEt)]$_2$ (1): Geometrical restraints have been applied for disordered parts of the ligand (see CIF). The unit cell contains four diethyl ether molecules close to a special position, which have been treated as a diffuse contribution to the overall scattering without specific atom positions by PLATON/SQUEEZE.[15]

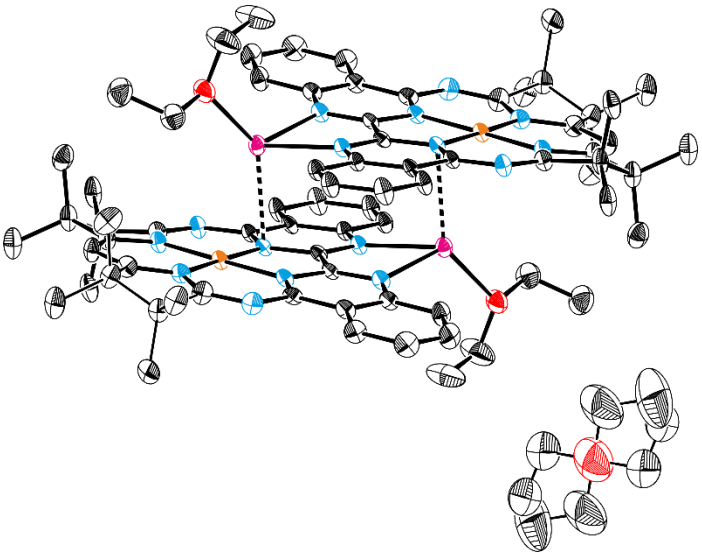

The above figure shows the ORTEP style representation of **1** with one equivalent of diethyl ether co-crystallized close to a special position, which has been treated as a diffuse contribution to the overall scattering without specific atom positions by PLATON/SQUEEZE[15] in the subsequent refinement process. Ellipsoids are shown at the 50% probability level. Hydrogen atoms are omitted for clarity.

Density Functional Theory calculations

Density Functional Theory (DFT) calculations were performed with the ORCA program package.[16] Geometry optimizations of the complexes were performed at the B3LYP[17-19] level of DFT. The all-electron Gaussian basis sets were those developed by the Ahlrich's group.[20-21] Triple-ζ quality basis sets (TZV(P)) with one set of polarization functions on the metals and on the atoms directly coordinated to the metal center were used.[21] For the carbon and hydrogen atoms, slightly smaller polarized split-valence SV(P) basis sets were used that were of double-ζ quality in the valence region and contained a polarizing set of d functions on the non-hydrogen atoms. Auxiliary basis sets used to expand the electron density in the resolution-of-the-identity (RI) approach were chosen,[22-23] where applicable, to match the orbital basis. SCF calculations were tightly converged (1×10^{-8} E_h in energy, 1×10^{-7} E_h in the density change, and 1×10^{-7} E_h in maximum element of the DIIS error vector). Geometry optimizations were carried out in redundant internal coordinates without imposing symmetry constraints. In all cases the geometries were considered converged after the energy change was less than 5×10^{-6} E_h, the gradient norm and maximum gradient element were smaller than 1×10^{-4} and 3×10^{-4} E_h $Bohr^{-1}$, respectively, and the root-mean square and maximum displacements of all atoms were smaller than 2×10^{-3} and 4×10^{-3} Bohr, respectively. Orbital/spin density plots were created using GaussView.[24]

Syntheses

[Co(Mabiq)Na(OEt$_2$)]$_2$ (1). Sodium (3.3 mg, 0.14 mmol) was added to a solution of Co(Mabiq) (86.2 mg, 0.14 mmol) in THF (10 mL) and the mixture was stirred for 48 h. The resultant dark red solution was filtered through celite and the solvent evaporated. The crude product was dissolved in ether and precipitated with hexane to give a dark red solid (80 mg, 80% yield). Single crystals were grown by slow evaporation of a concentrated solution of **1** in Et_2O.

Anal. Calcd. for Co(Mabiq)Na(OEt$_2$), $C_{37}H_{43}Co\ N_8NaO$: C, 63.69; H, 6.21; N, 16.06. Found: C, 63.51; H, 6.19; N, 15.95.

UV-Vis λ_{max} (nm (ε, $M^{-1}\ cm^{-1}$)) in THF: 340 (3.6 x 10^4), 401 (2.6 x 10^4), 442 (1.6 x 10^4), 534 (1.5 x 10^4), 870 (3.4 x 10^3), 1038 (2.1 x 10^3), 1206 (1.9 x 10^3).

[Co(Mabiq)(THF)](PF$_6$) (3). [Co(CH_3CN)$_6$](PF_6)$_2$ (105 mg, 0.18 mmol) was added to a suspension of HMabiq (96 mg, 0.18 mmol) and triethylamine (26 µL, 0.19 mmol) in MeCN (5 mL). The suspension was stirred overnight and the resultant brown mixture was filtered through celite. After evaporation of the solvent, the crude product was dissolved in DCM and precipitated with hexane to give a red solid (120 mg, 82% yield). Single crystals were obtained by slow diffusion of pentane into a concentrated solution of **3** in THF.

Anal. Calcd. for $C_{37}H_{41}CoF_6N_8OP$: C, 54.35; H, 5.05; N, 13.70. Found: C, 54.24; H, 5.08; N, 13.46.

ESI-MS(+) (*m/z*): 600.65 [M-(THF + PF_6)]$^+$.

UV-Vis λ_{max} (nm (ε, $M^{-1}\ cm^{-1}$)) in THF: 316 (3.1 x 10^4), 429 (9.5 x 10^3), 570 (3.5 x 10^3), 607 (2.7 x 10^3), 658 (1.3 x 10^3).

General procedure for reactions of 1 and 2 with acid (*p*CA, benzoic acid)

All reactions were carried out in an inert atmosphere (argon) glovebox. 0.5 mL of **1** or **2** (0.015 M solution in THF-d_8) were placed in a J-Young NMR tube and frozen. Subsequently, 20 or 100 µL (1 or 5 equiv.) of a 0.36 M solution of acid in THF-d_8 were added to the frozen sample. The NMR tube was sealed and kept frozen until the measurement of the NMR spectrum. Aliquots of each reaction mixture were analyzed by absorption spectroscopy and ESI mass spectrometry.

Alternatively, 0.5 mL of **1** or **2** (0.015 M solution in THF) were placed in a vial and 20 or 100 µL (1 or 5 equiv.) of a 0.36 M solution of acid in THF were added. The mixtures were stirred for 30 min and analyzed by absorption spectroscopy and ESI mass spectrometry.

Isolation of [2-H_2] from the 1/benzoic acid reaction

Compound **1** (70 mg, 0.1 mmol) was dissolved in THF (5 mL) and a solution of benzoic acid (61 mg, 0.5 mmol) in THF (1 mL) was added. The reaction mixture was stirred for 30 min, filtered and the solvent removed in vacuo. The solid was subsequently washed with MeCN to remove excess benzoic acid. The remaining purple solid was a mixture of **2** and **[2-H_2]**, from which **[2-H_2]** was separated by column chromatography (THF:hexane = 1:6, R_f = 0.43, silica gel , pore size 60 Å, 230-400 mesh particle size, 40-63 µm) as a purple solid (21 mg, 35% yield). Single crystals of **[2-H_2]** were obtained by slow diffusion of pentane into a concentrated solution of **[2-H_2]** in THF.

^{1}H NMR (400 MHz, benzene-d_6, 25 °C, TMS): δ= 1.16 (s, 3H, CH_3, H_a), 1.26 (s, 3H, CH_3, H_a), 1.27 (s, 3H, CH_3, H_a), 1.28 (s, 3H, CH_3, H_a), 1.33 (s, 3H, CH_3, H_a), 1.34 (s, 3H, CH_3, H_a), 1.38 (s, 3H, CH_3, H_a), 1.39 (s, 3H, CH_3, H_a), 6.52 (s, 1H, NH, H_e), 6.56 (dd, J = 8.0, 1.1 Hz, 1H, CH, H_c), 6.89 - 6.82 (m, 1H, CH, H_d), 7.22 (ddd, J = 8.1, 6.9, 1.1 Hz, 1H, CH, $H_{d'}$), 7.30 (s, 1H, CH, H_b), 7.34 (m, 1H, CH, H_d),

7.47 (s, 1H, CH, H_f), 7.76 (ddd, *J* = 8.2, 6.9, 1.4 Hz, 1H, CH, $H_{d'}$), 8.14 (d, *J* = 8.1 Hz, 1H, CH, $H_{c'}$), 8.82 (dd, *J* = 7.8, 1.4 Hz, 1H, CH, H_c), 9.17 (dd, *J* = 8.2, 1.3 Hz, 1H, CH, $H_{c'}$).

Table S1. Crystallographic data for **3** and **1** at 100K.

	3	**1**
Empirical formula	$4(C_{37}H_{41}CoN_8O)$, $4(F_6P)$, C_4H_8O	$C_{74}H_{86}Co_2N_{16}Na_2O_2$
Formula weight	3342.82	1395.43
Crystal system	monoclinic	monoclinic
Space group	*C* 2/*c*	*P* 2_1/*c*
a (Å)	71.25(3)	12.6857(8)
b (Å)	10.283(4)	14.0773(10)
c (Å)	20.132(8)	21.3596(13)
α (°)	90	90
β (°)	91.821(3)	99.336(2)
γ (°)	90	90
Volume ($Å^3$)	14743(10)	3763.9(4)
Z	4	2
ρ_{calc} (mg/mm^3)	1.506	1.231
μ (mm^{-1})	0.585	0.507
F(000)	6928	1468
Reflections collected	57304	116385
Independent refl., R_{int}	12999, 0.0955	6647, 0.0796
Data/restraints/parameters	12999/262/1141	6647/137/502
Goodness-of-fit on F^2	1.057	1.137
Final R_1 indexes [$I \geq 2\sigma(I)$]	0.0594	0.0643
Final wR_2 indexes [all data]	0.1425	0.1698
$\Delta\rho_{min,max}$ (e $Å^{-3}$)	0.741/-0.651	0.906/-0.538

Table S2. Select bond distances for **3** and **1**.

	3[a]	**1**
Co1–N1	1.915(3) (Co2–N10 1.920(3))	1.890(3)
Co1–N2	1.918(3) (Co2–N9 1.913(3))	1.890(3)
Co1–N3	1.899(3) (Co2–N12 1.898(3))	1.868(3)
Co1–N4	1.896(3) (Co2–N11 1.887(4))	1.878(3)
N3–C13	1.347(5) (N12–C52 1.350(5))	1.361(5)
C13–C14	1.388(6) (C52–C51 1.391(6))	1.392(6)
C14–C15	1.387(6) (C51–C50 1.379(6))	1.374(6)
N4–C15	1.354(5) (N11–C50 1.350(5))	1.367(5)
C9–N2	1.341(5) (N9–C56 1.346(5))	1.355(5)
N2–C2	1.394(5) (N9–C38 1.380(5))	1.400(5)
C2–N6	1.299(5) (C38–N13 1.300(5))	1.347(5)
N6–C3	1.370(5) (N13–C62 1.380(5))	1.365(5)
C2–C1	1.476(5) (C38–C39 1.491(6))	1.422(5)
C19–N1	1.345(5) (C46–N10 1.348(5))	1.350(5)
N1–C1	1.377(5) (N10–C39 1.376(5))	1.396(5)
C1–N5	1.303(5) (C39–N14 1.300(5))	1.328(5)
N5–C25	1.378(5) (N14–C40 1.374(5))	1.373(5)
Na1–N5		2.335(5)
Na1–N6		2.381(5)
Na1–N1a		2.676(4)

[a] the asymmetric unit of **3** contains two independent molecules. The corresponding values for the second molecule are therefore are also given, in parentheses.

Table S3. DFT-derived (B3LYP, UKS) Löwdin atomic charges and spin populations for the monomeric unit of **1**.

LOEWDIN ATOMIC CHARGES AND SPIN POPULATIONS

---

0 Co:	0.203739	-0.816272
1 Na:	0.561383	0.002865
2 O :	-0.510054	-0.000041
3 N :	-0.524272	0.171834
4 N :	-0.334200	0.015500
5 N :	-0.463625	-0.013663
6 N :	-0.357907	-0.014087
7 N :	-0.355380	-0.017871
8 N :	-0.463054	-0.015552
9 N :	-0.337051	0.019538
10 N :	-0.524120	0.169344
11 C :	0.266964	0.145579
12 C :	0.144285	-0.013562
13 C :	-0.135262	0.067259
14 C :	-0.108143	-0.007405
15 C :	-0.147193	0.071894
16 C :	-0.088307	-0.000909
17 C :	-0.021925	0.042405
18 C :	0.295532	0.090286
19 C :	0.309011	0.092826
20 C :	-0.041985	0.001927
21 C :	-0.289496	0.000492
22 C :	-0.288040	0.005560
23 C :	-0.050619	-0.002990
24 C :	-0.289918	0.014472
25 C :	-0.296877	0.003772
26 C :	0.136131	0.268386
27 C :	-0.168528	-0.077270
28 C :	0.136224	0.269745
29 C :	-0.050629	-0.002919
30 C :	-0.290046	0.014553
31 C :	-0.296607	0.003799
32 C :	-0.041944	0.001623
33 C :	-0.289465	0.000704
34 C :	-0.288124	0.006040
35 C :	0.306546	0.102113
36 C :	0.294418	0.095657
37 C :	-0.021523	0.040438
38 C :	-0.088203	0.001405

39	C :	-0.147120	0.069999
40	C :	-0.108716	-0.004848
41	C :	-0.137463	0.065752
42	C :	0.143635	-0.011571
43	C :	0.268444	0.142056
44	C :	-0.313234	0.000085
45	C :	0.013416	0.000023
46	C :	0.014440	0.000014
47	C :	-0.323159	-0.000006
48	H :	0.120654	-0.002136
49	H :	0.114837	0.000230
50	H :	0.116021	-0.002360
51	H :	0.136615	0.000076
52	H :	0.115021	0.000047
53	H :	0.122067	0.000094
54	H :	0.107191	0.000208
55	H :	0.120781	-0.000118
56	H :	0.115629	-0.000112
57	H :	0.109934	0.000536
58	H :	0.117140	-0.000380
59	H :	0.110118	0.002634
60	H :	0.111585	-0.000057
61	H :	0.114308	0.000239
62	H :	0.111160	-0.000079
63	H :	0.112454	0.000519
64	H :	0.122693	0.002391
65	H :	0.117146	-0.000371
66	H :	0.111543	-0.000093
67	H :	0.110162	0.002592
68	H :	0.112290	0.000542
69	H :	0.110987	-0.000074
70	H :	0.114207	0.000244
71	H :	0.122096	0.000084
72	H :	0.114910	0.000038
73	H :	0.106900	0.000229
74	H :	0.120632	-0.000139
75	H :	0.109887	0.000551
76	H :	0.115485	-0.000104
77	H :	0.136548	0.000004
78	H :	0.116028	-0.002297
79	H :	0.114988	0.000146
80	H :	0.121690	-0.002084
81	H :	0.142112	-0.000010
82	H :	0.139441	0.000013
83	H :	0.134789	0.000010
84	H :	0.113135	0.000000

85	H :	0.114371	0.000009
86	H :	0.129079	-0.000004
87	H :	0.115068	0.000001
88	H :	0.127504	0.000001
89	H :	0.129184	-0.000000
90	H :	0.119633	0.000001

Table S4. DFT-optimized (B3LYP, UKS) geometry (.XYZ format) for the monomeric unit of **1**.

CARTESIAN COORDINATES (ANGSTROEM)

Co	0.097797	0.117993	-0.168999
Na	0.374752	-5.527592	-0.230111
O	0.626188	-7.791673	-0.561952
N	-1.122565	-3.790384	-0.248507
N	-1.121508	-1.363234	-0.259888
N	-3.176049	-0.180010	-0.406245
N	-1.350033	1.361575	-0.124509
N	1.415329	1.497530	-0.069812
N	3.391791	0.138629	-0.264154
N	1.455849	-1.236551	-0.198962
N	1.690660	-3.651472	-0.164765
C	-0.485507	-2.601909	-0.231377
C	-2.486877	-3.787959	-0.301818
C	-3.204564	-5.012849	-0.315473
C	-4.591788	-5.024234	-0.375702
C	-5.314580	-3.816876	-0.424975
C	-4.629296	-2.603736	-0.412952
C	-3.224493	-2.571478	-0.351031
C	-2.463802	-1.322865	-0.332869
C	-2.654241	1.012868	-0.325424
C	-3.528487	2.253022	-0.523069
C	-4.955999	2.081261	0.010367
C	-3.598854	2.501364	-2.051475
C	-2.657706	3.338275	0.210293
C	-2.976879	3.393210	1.726966
C	-2.787972	4.758023	-0.362450
C	-1.268802	2.722410	0.053531
C	-0.070376	3.414864	0.162547
C	1.194207	2.843017	0.098311
C	2.508160	3.592551	0.311279
C	2.750603	3.683935	1.840413
C	2.521021	5.016175	-0.266592
C	3.513043	2.595690	-0.374750
C	4.923988	2.562422	0.224691
C	3.629471	2.846836	-1.899486
C	2.754639	1.276617	-0.210239
C	2.791425	-1.066556	-0.214680
C	3.668286	-2.236327	-0.186772
C	5.071200	-2.135086	-0.187725
C	5.868858	-3.277195	-0.151367
C	5.263702	-4.547608	-0.111248

C	3.880004	-4.668534	-0.111321
C	3.049512	-3.517708	-0.152388
C	0.942159	-2.531519	-0.192741
C	1.300112	-7.160928	-2.791343
C	1.084221	-8.310705	-1.822687
C	0.397005	-8.785925	0.452822
C	-0.920650	-9.535136	0.289249
H	-2.640887	-5.952434	-0.278379
H	-5.126493	-5.980131	-0.385331
H	-6.407479	-3.831734	-0.472885
H	-5.165342	-1.654015	-0.451355
H	-4.977018	1.735797	1.055767
H	-5.494799	1.331109	-0.591283
H	-5.510644	3.035972	-0.054732
H	-4.043801	1.620793	-2.545848
H	-2.599139	2.668641	-2.488634
H	-4.228997	3.378061	-2.283511
H	-2.929628	2.393210	2.191837
H	-3.982131	3.812577	1.910888
H	-2.240744	4.035834	2.240851
H	-2.414309	4.835156	-1.396226
H	-2.223550	5.482281	0.251549
H	-3.844517	5.083381	-0.351804
H	-0.127397	4.493593	0.319536
H	2.779281	2.685625	2.310400
H	1.932138	4.252783	2.315067
H	3.700414	4.200201	2.067166
H	3.536738	5.449228	-0.210488
H	1.856872	5.680790	0.314311
H	2.189642	5.050243	-1.316880
H	5.555379	1.857267	-0.340365
H	4.927975	2.231162	1.274823
H	5.393687	3.562409	0.170355
H	4.184748	2.015537	-2.366522
H	4.175868	3.783647	-2.107939
H	2.639161	2.908121	-2.383508
H	5.516248	-1.139094	-0.216454
H	6.959242	-3.187173	-0.151615
H	5.887035	-5.447721	-0.078336
H	3.406268	-5.656098	-0.074751
H	2.056483	-6.448304	-2.414576
H	0.357823	-6.616789	-2.986972
H	1.663758	-7.550650	-3.758176
H	0.338798	-9.021431	-2.227031
H	2.027962	-8.867273	-1.654761
H	0.405630	-8.234462	1.409005

H	1.254648	-9.486405	0.467310
H	-1.773639	-8.833663	0.277301
H	-1.058625	-10.228022	1.138876
H	-0.949133	-10.134955	-0.637051

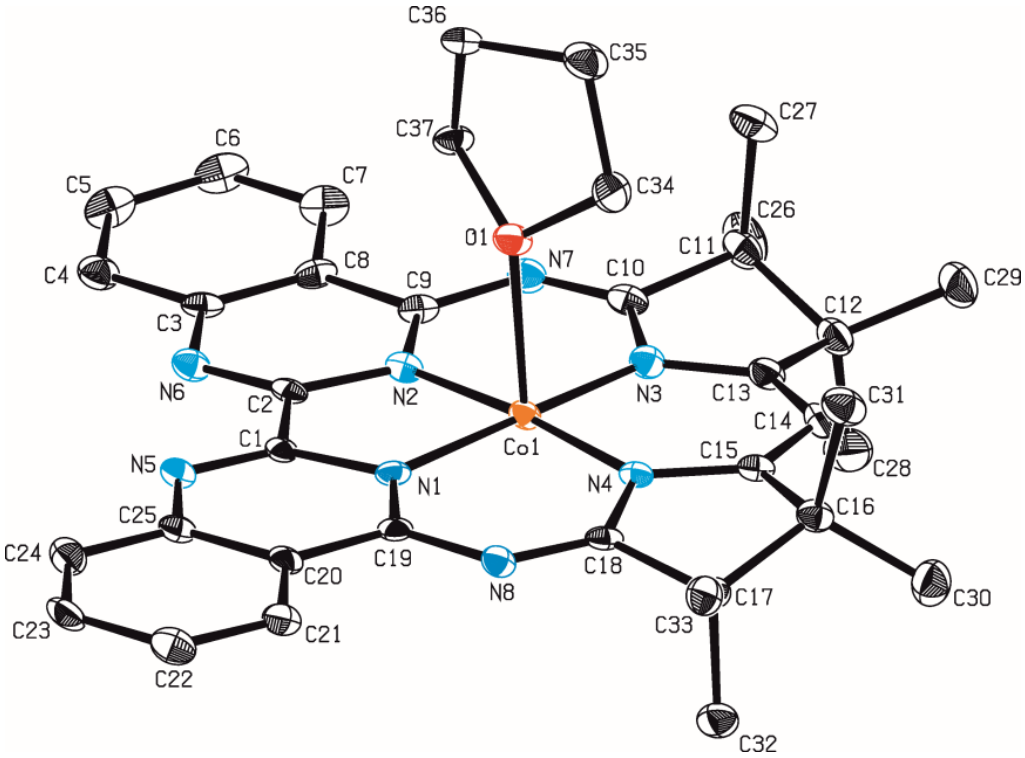

Figure S1. ORTEP style representation of **3** (one of two molecules in the asymmetric unit). Ellipsoids are shown at the 50% probability level. Hydrogen atoms are omitted for clarity.

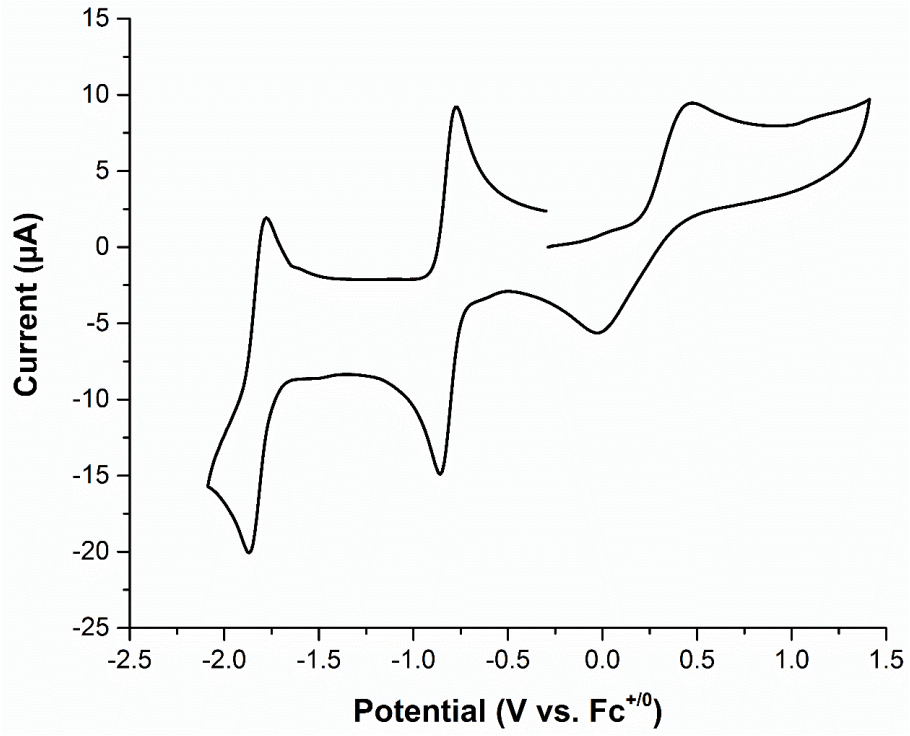

Fig. S2. Cyclic voltammogram of **3** (0.84 mM) in MeCN; 0.1 M $[N(n\text{-}Bu)_4]PF_6$; scan rate: 0.1 V/s.

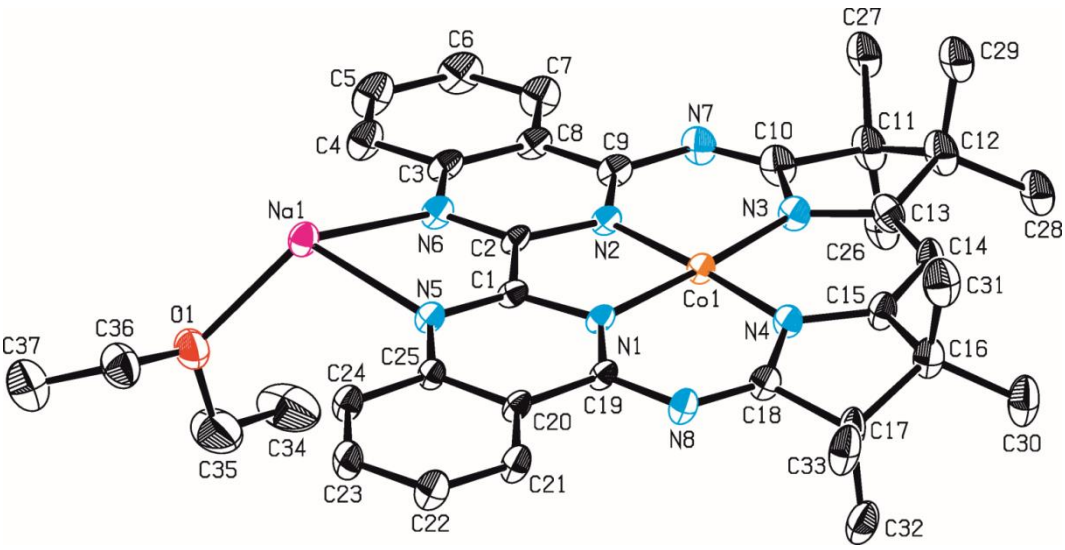

Figure S3. ORTEP style representation of the monomeric unit of **1**. Ellipsoids are shown at the 50% probability level. Hydrogen atoms omitted for clarity.

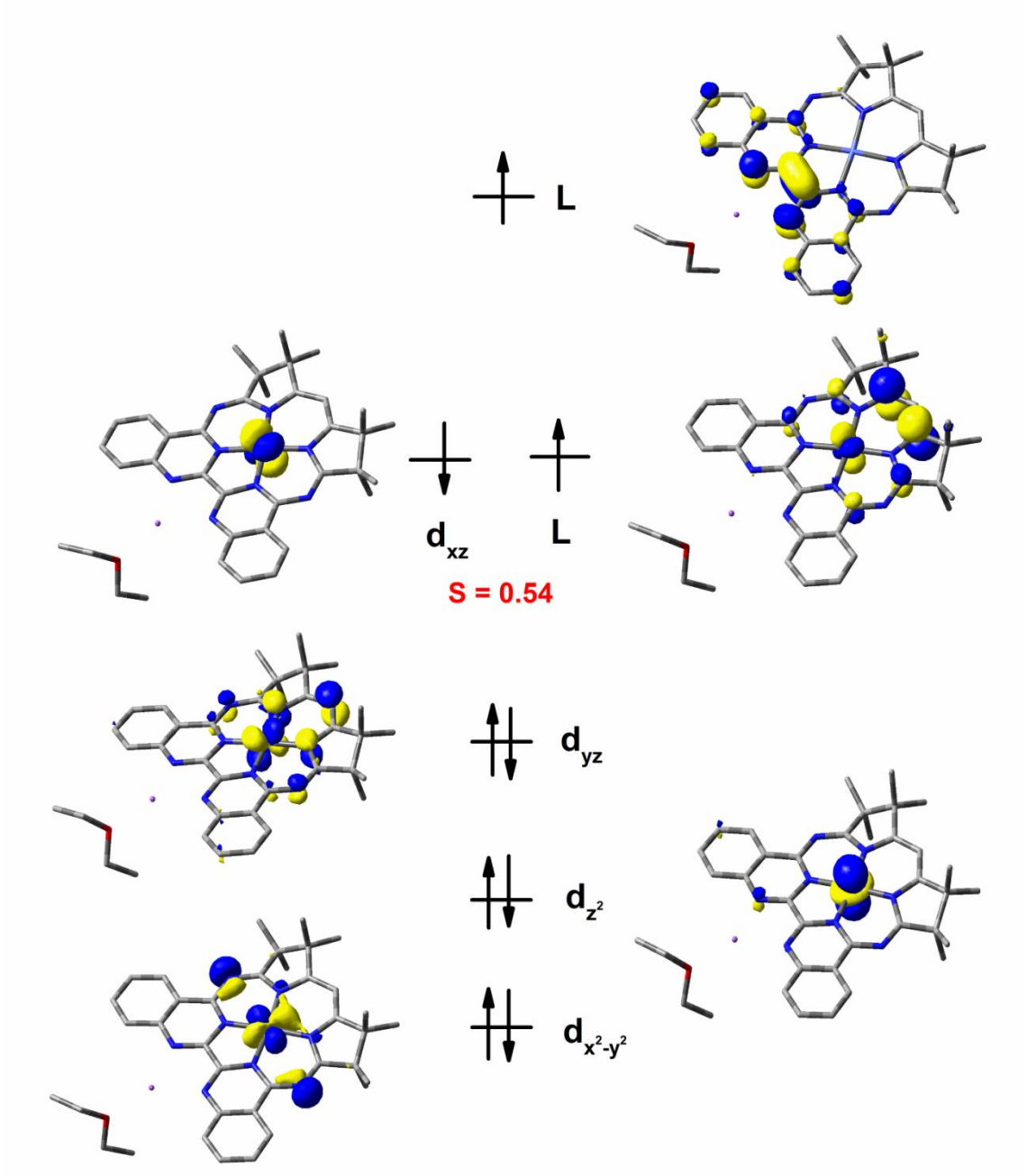

Figure S4. DFT-derived (B3LYP) qualitative molecular orbital diagram of the monomeric unit ([Co(Mabiq)Na(OEt_2)]) of **1**.

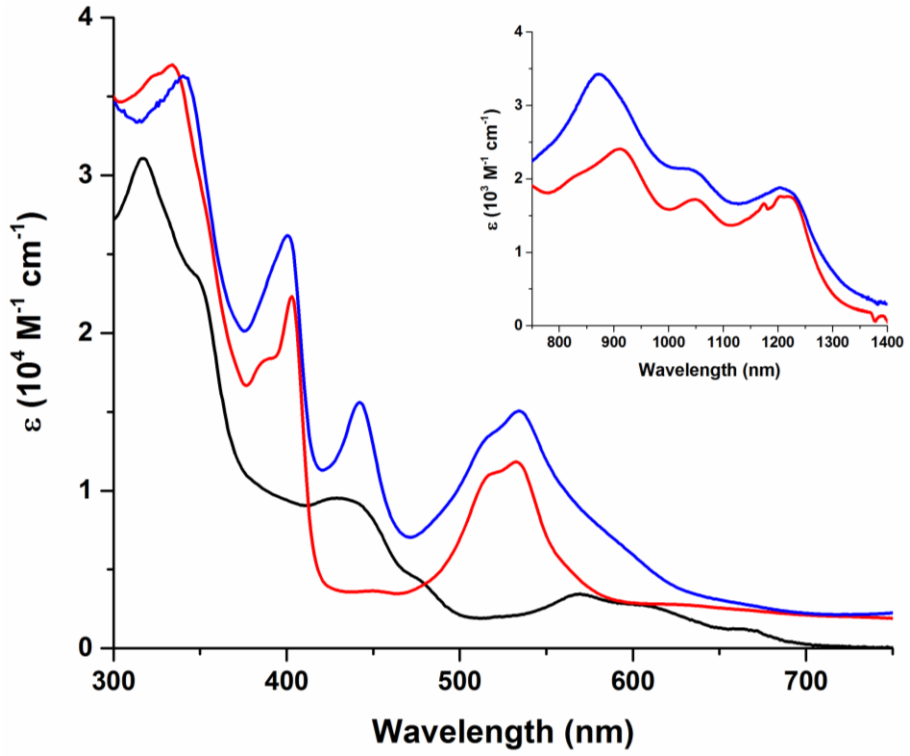

Fig. S5. Electronic spectra of **1** (blue), **2** (red) and **3** (black) in THF. Inset NIR region of the spectra of **1** and **2**.

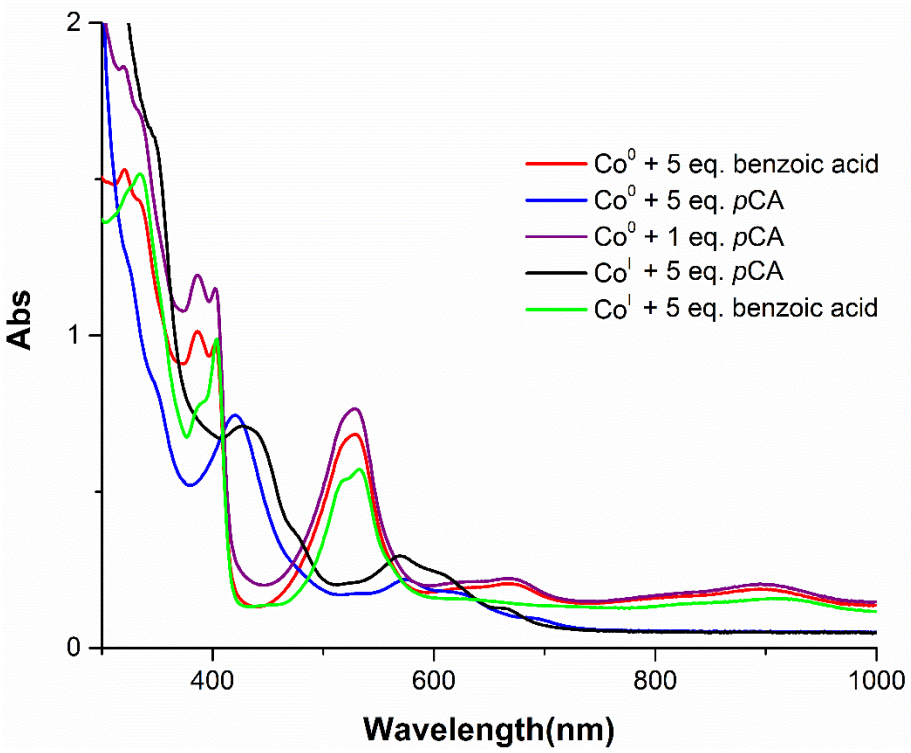

Figure S6. UV-vis spectra of the reaction products of **1** and **2** with *p*CA and benzoic acid.

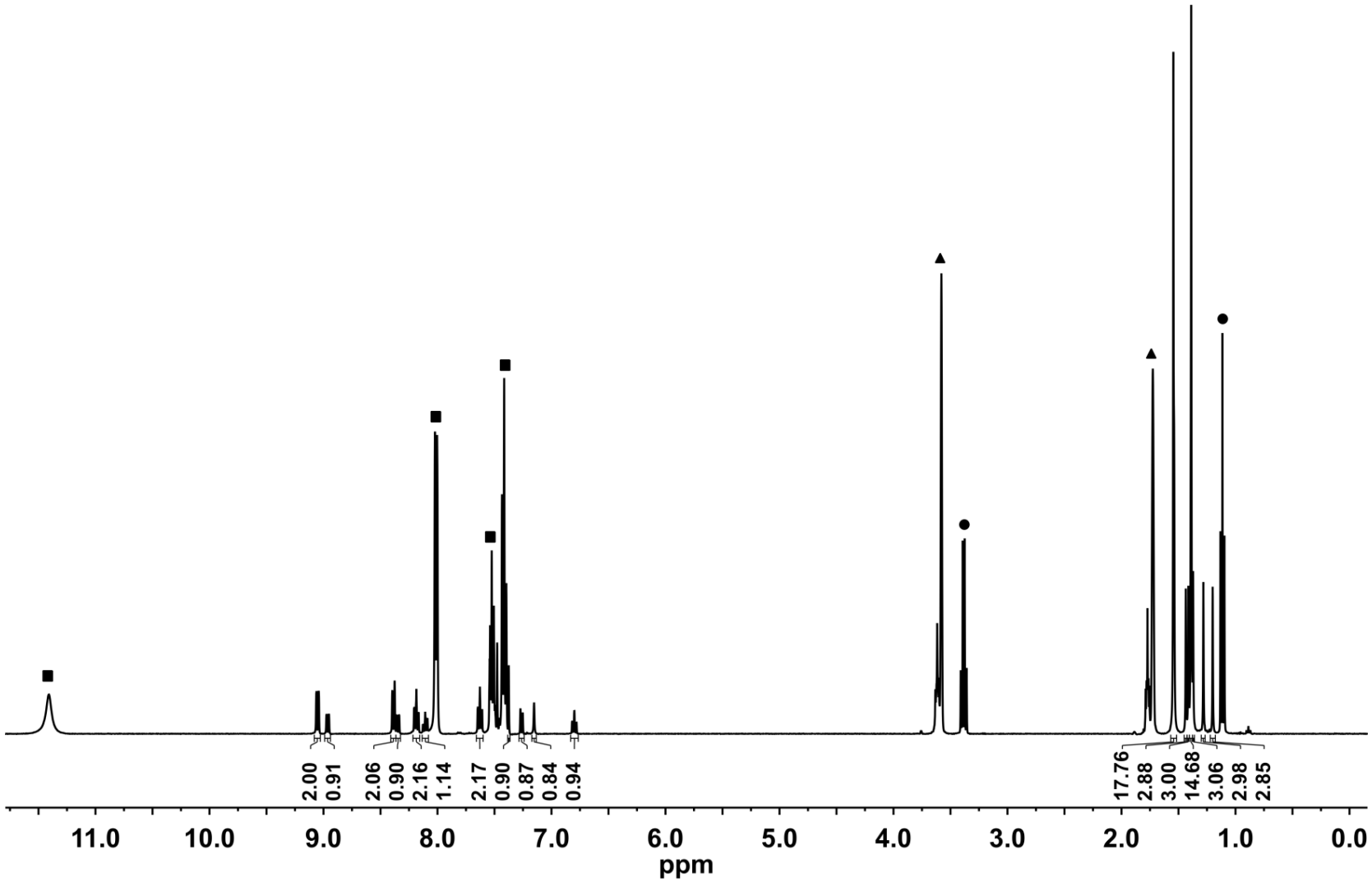

Figure S7. Full ^{1}H NMR spectrum for the product of **1** ([Co] = 0.015 mM) plus 5 equiv. benzoic acid in THF-d_8; ■ benzoic acid, ● Et_2O, ▲ THF-d_8.

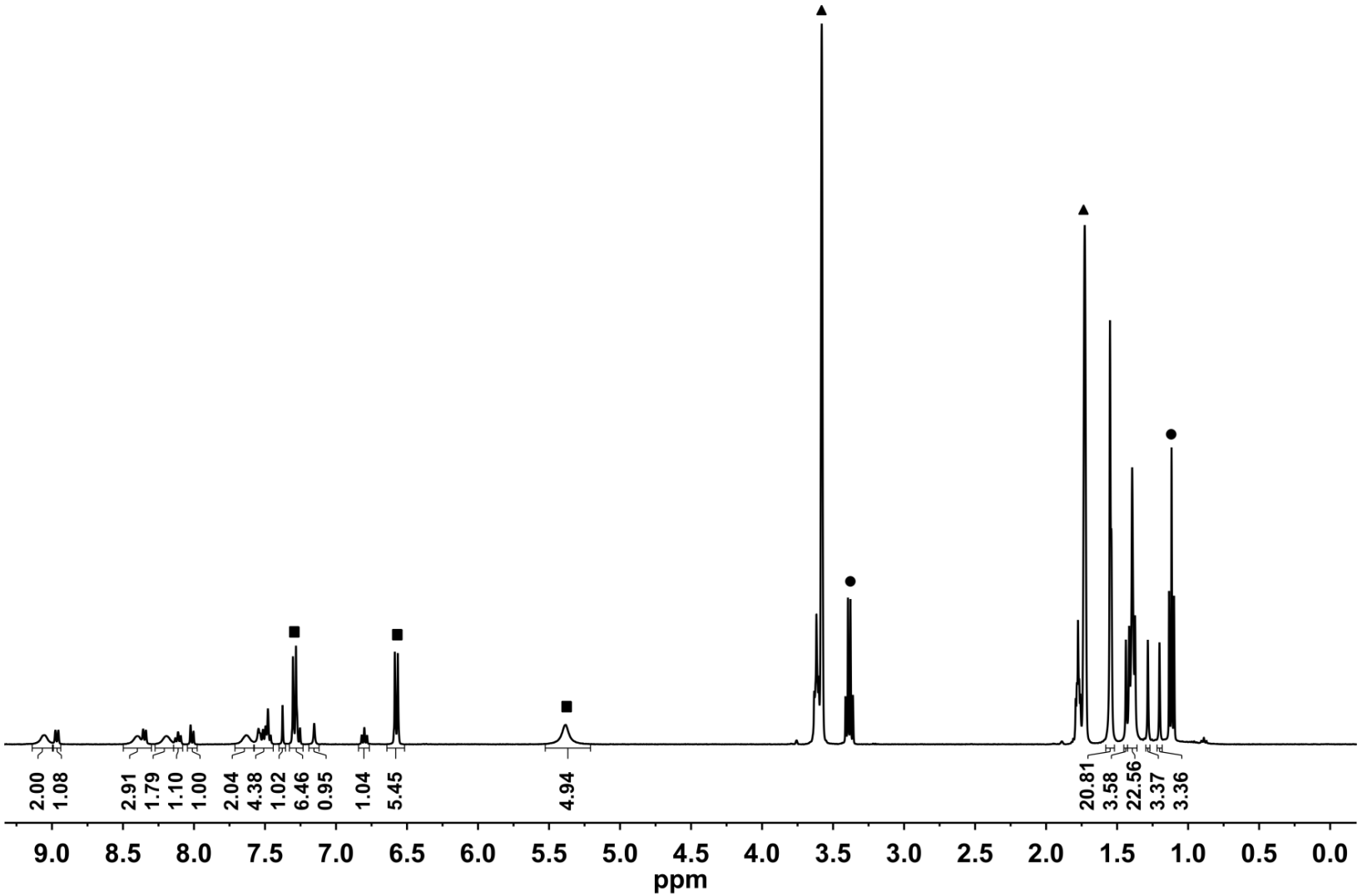

Figure S8. Full ^{1}H NMR spectrum for the product of **1** ([Co] = 0.015 mM) plus 1 equiv. *p*-cyanoaniline in THF-d_8; ■ *p*CA, ● Et_2O, ▲ THF-d_8.

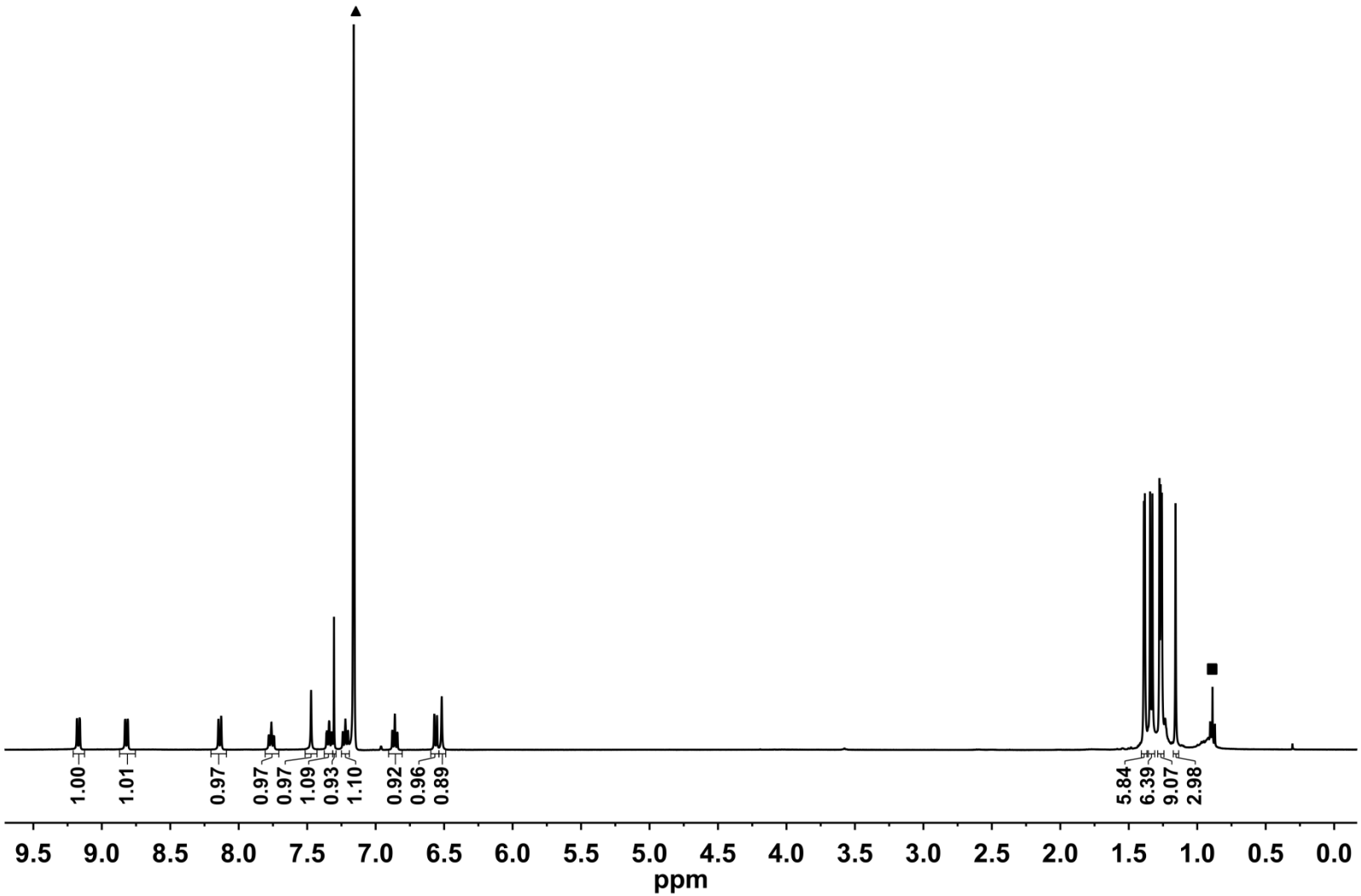

Figure S9. Full ^{1}H NMR spectrum of. [**2-H$_2$**] in benzene-d$_6$; ▲ benzene-d$_6$, ■ hexane.

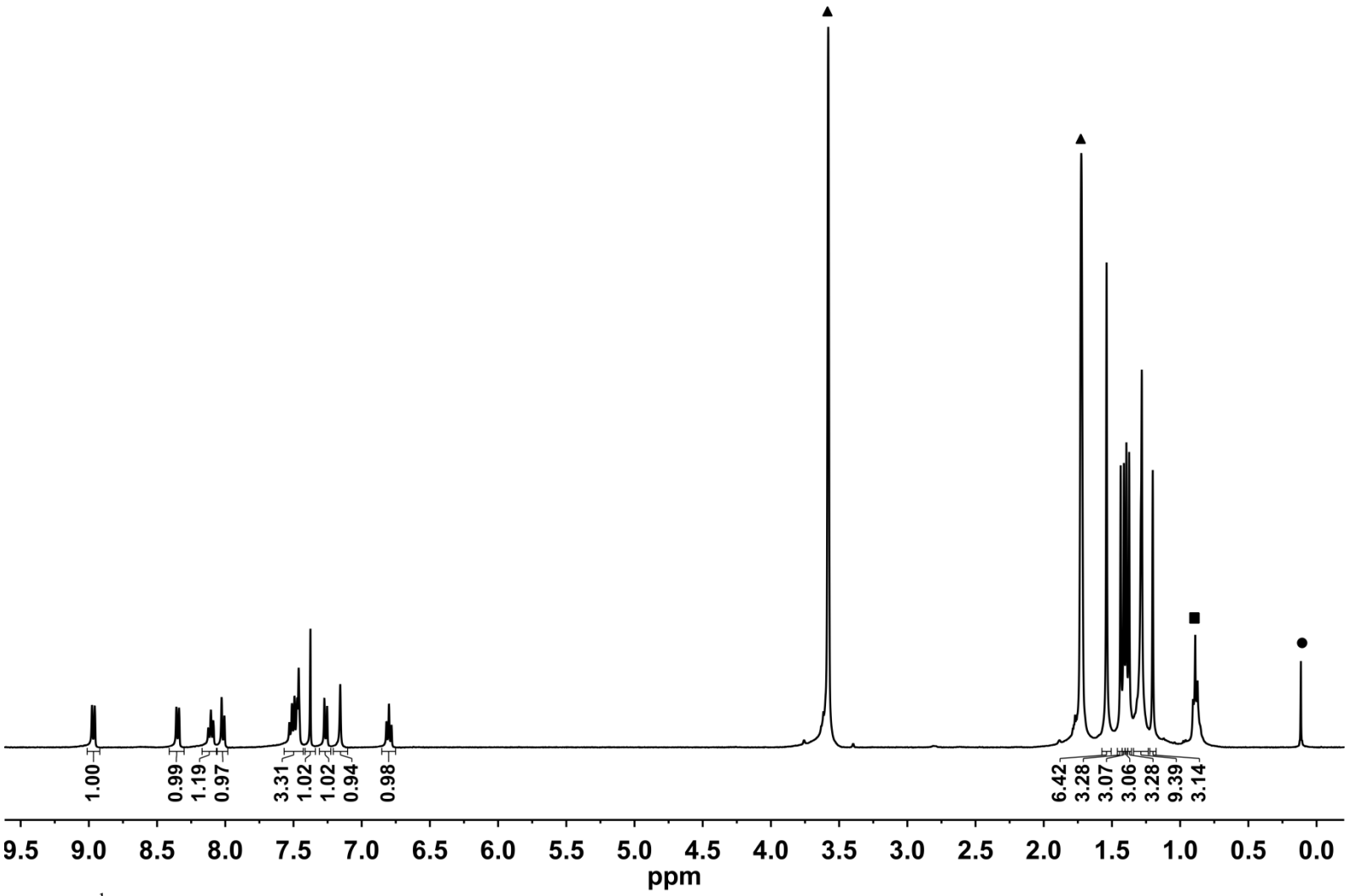

Figure S10. Full ^{1}H NMR spectrum of. [**2-H$_2$**] in THF-d$_8$; ▲ THF-d$_8$, ■ hexane, ▲silicon grease.

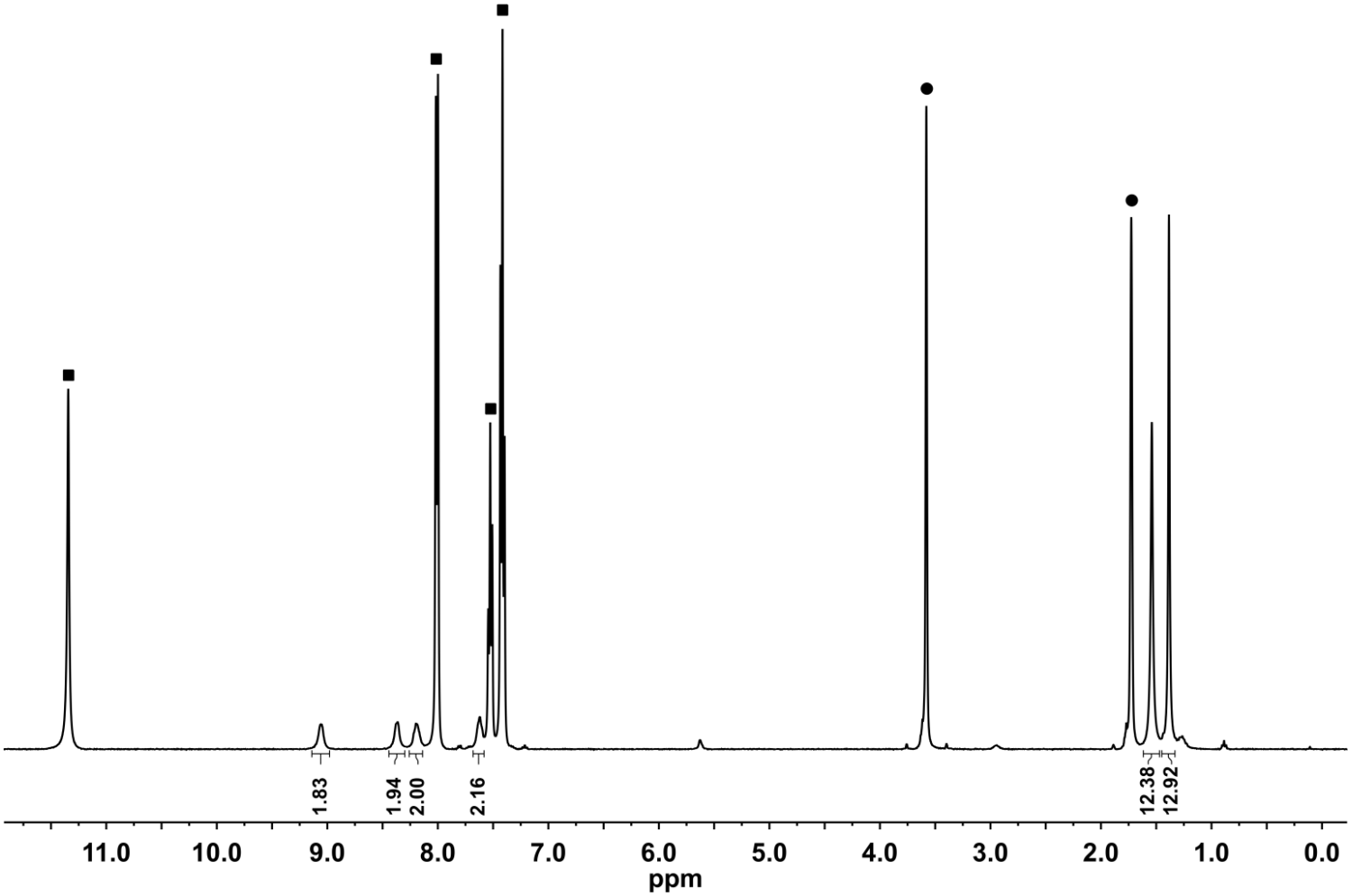

Figure S11. ^{1}H NMR spectrum of a mixture of **2** and 5 equiv. benzoic acid in THF-d_8; ■ benzoic acid, ● THF-d_8.

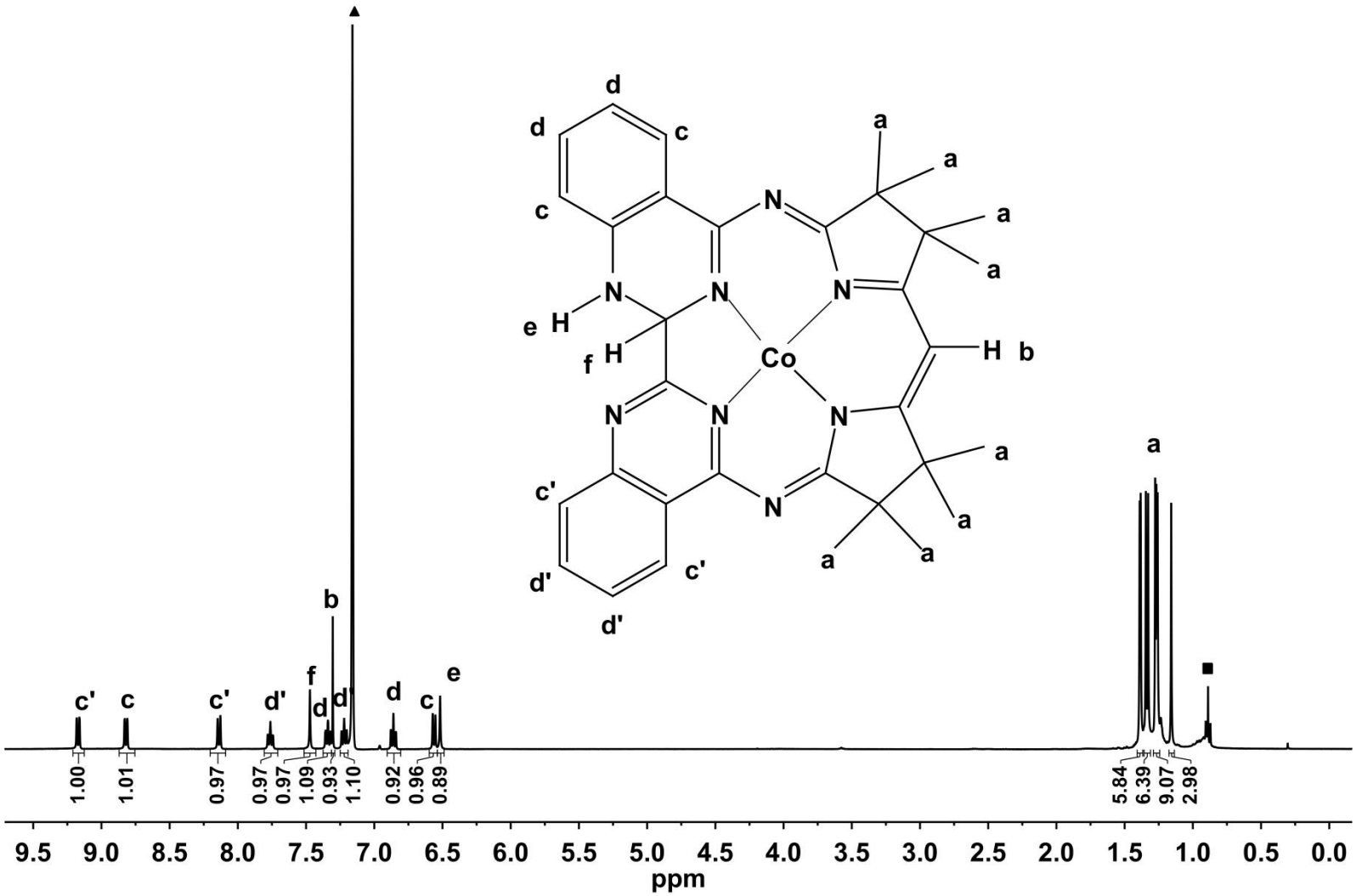

Figure S12. ^{1}H NMR spectrum of. [**2-H$_2$]** including proton assignments; ▲ benzene-d$_6$, ■ hexane.

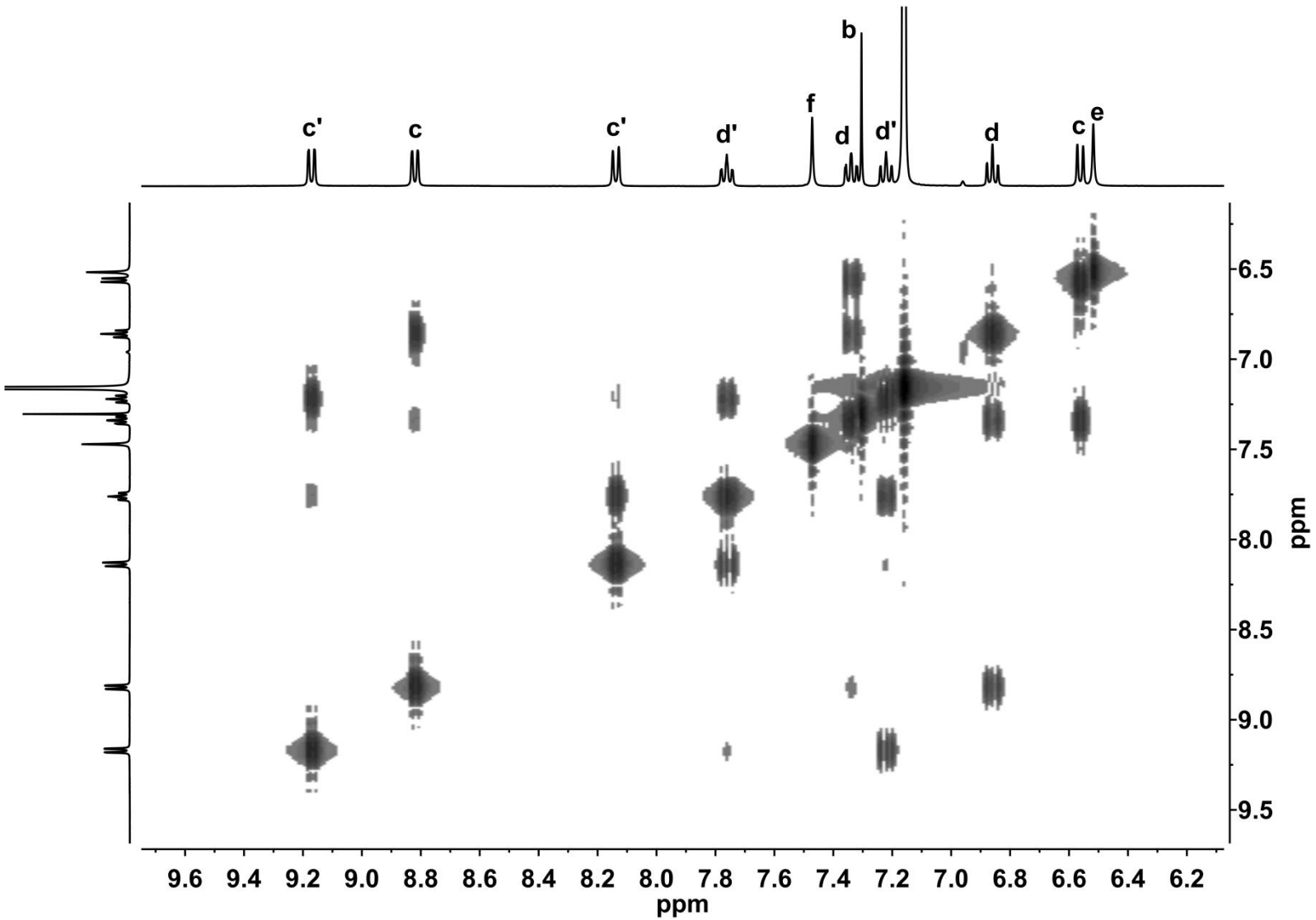

Figure S13. COSY NMR spectrum of. [**2-H$_2$**] in benzene-d$_6$.

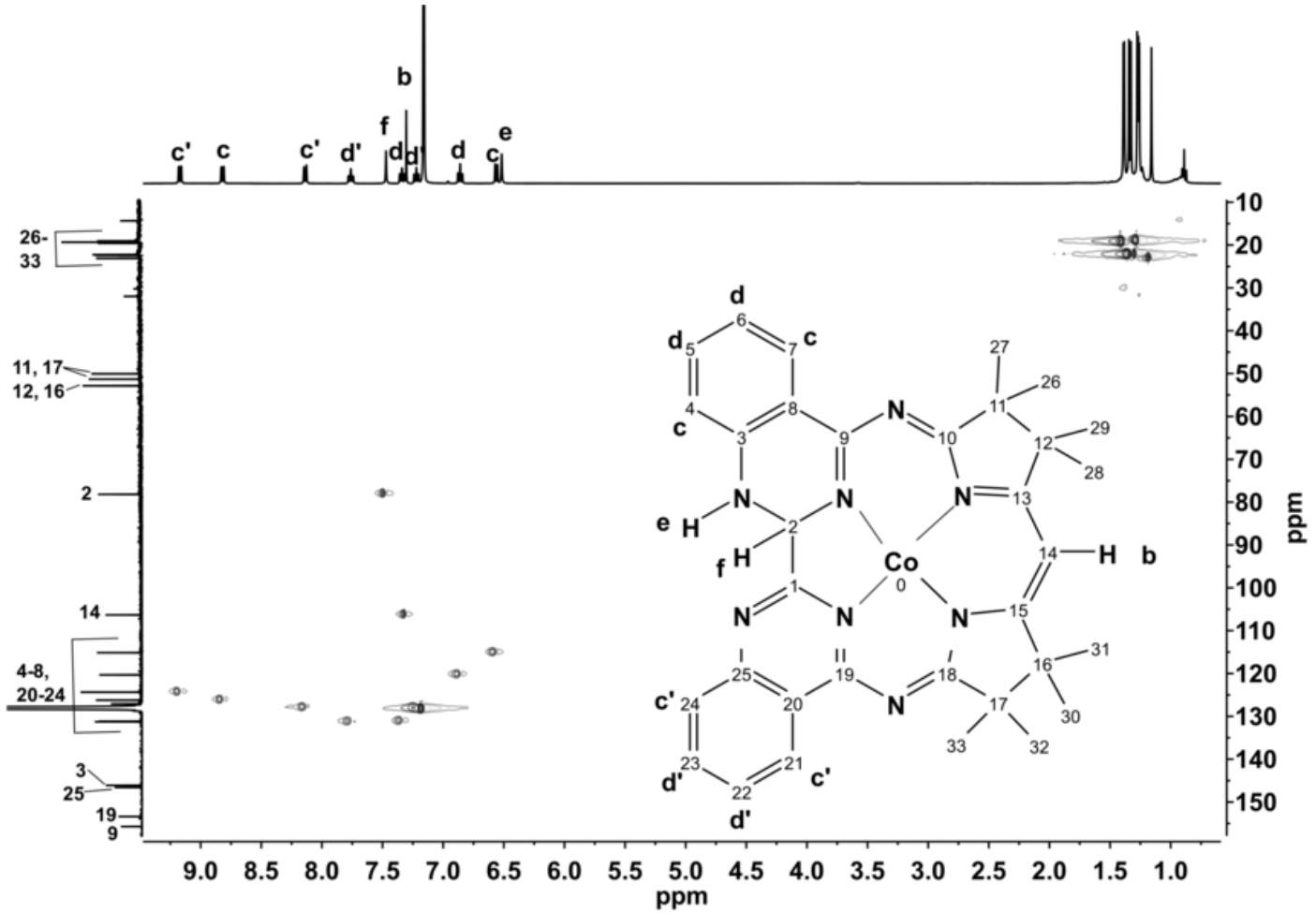

Figure S14. HSQC NMR spectrum of. [**2-H$_2$**] in benzene-d$_6$. The HSQC NMR spectrum of [**2-H$_2$**] shows, that the proton signal at 6.52 ppm (e) is not coupled to a carbon atom, such that the proton can be assigned to an N-H proton. In contrast, the proton resonance at 7.47 ppm (f) can be assigned to a C-bound proton.

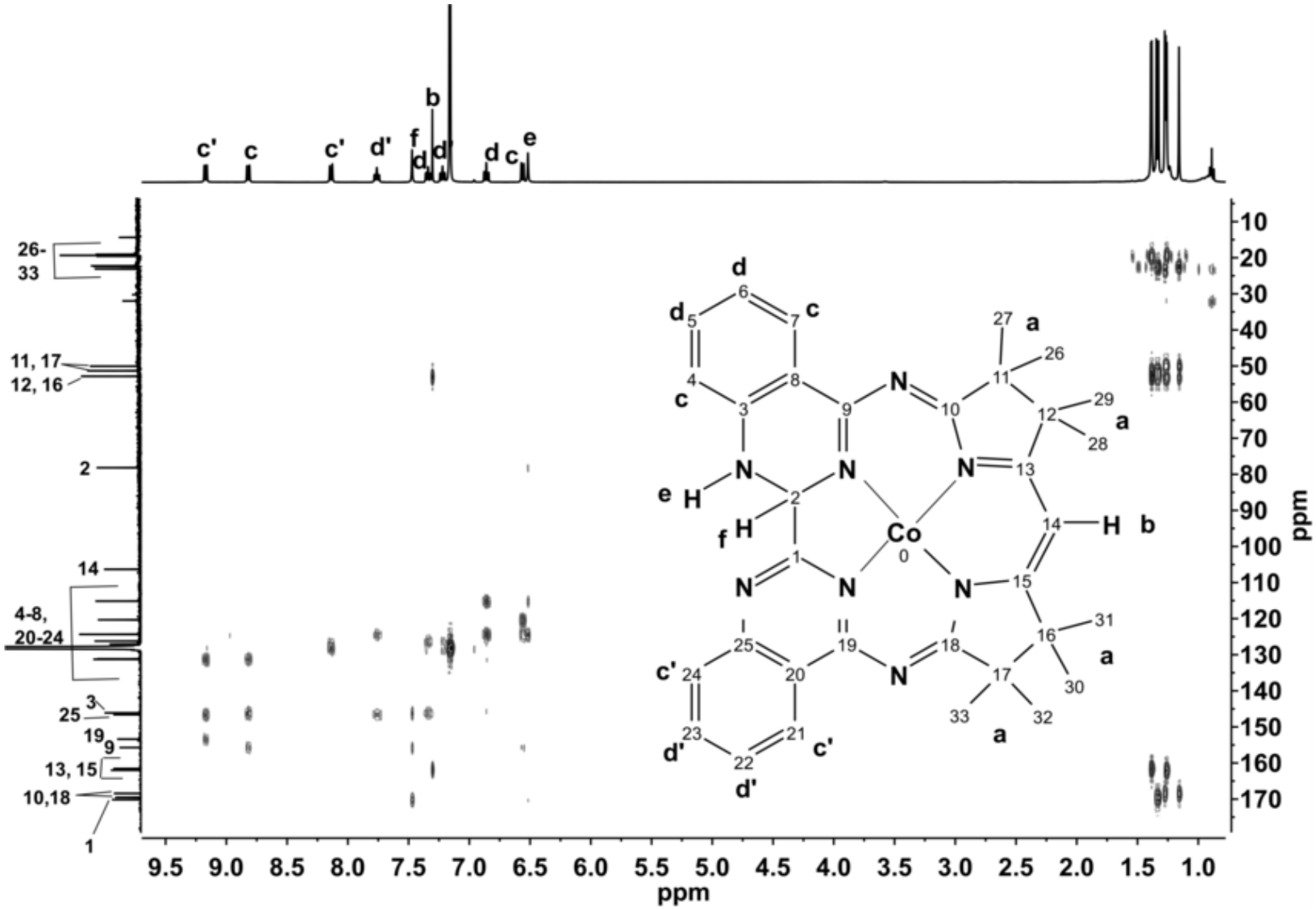
c'
c
c'
d'
f
d
b
d'
d
c
e
26-
33
11, 17
12, 16
2
14
4-8,
20-24
3
25
19
9
13, 15
10,18
1
9.5 9.0 8.5 8.0 7.5 7.0 6.5 6.0 5.5 5.0 4.5 4.0 3.5 3.0 2.5 2.0 1.5 1.0
ppm
10 20 30 40 50 60 70 80 90 100 110 120 130 140 150 160 170
ppm
Co
N
H
a
b
c
c'
d
d'
e
f

Figure S15. HMBC NMR spectrum of. **[2-H_2]** in benzene-d_6.

The proton resonance at 7.30 ppm (b) in the HMBC NMR spectrum of **[2-H_2]** could be assigned to a H atom bound to C14, as only coupling of this resonance to quaternary carbon atoms (C12, 13, 14, 16) is observed. The quaternary carbon atom signals couple to the proton signals of the Mabiq methyl groups, justifying the assignment of the singlet at 7.30 ppm to the diketiminate proton. The proton signal at 7.47 ppm (f) also is coupled solely to quaternary protons, indicating that the proton is attached to C1 or C2. The proton signal at 6.52 ppm (NH, e) is coupled to resonances corresponding to the aromatic C-H atoms and the carbon atom bound to H_f, and is therefore assigned to a proton bound to a bpm nitrogen atom.

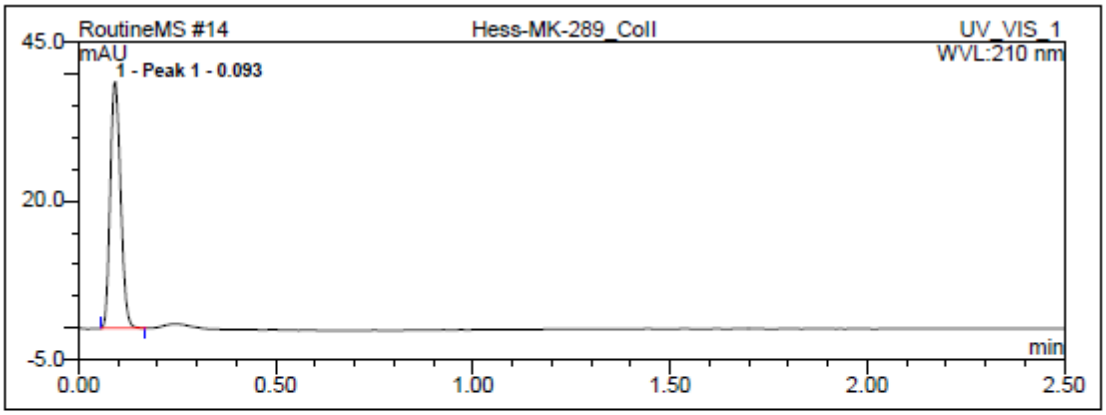

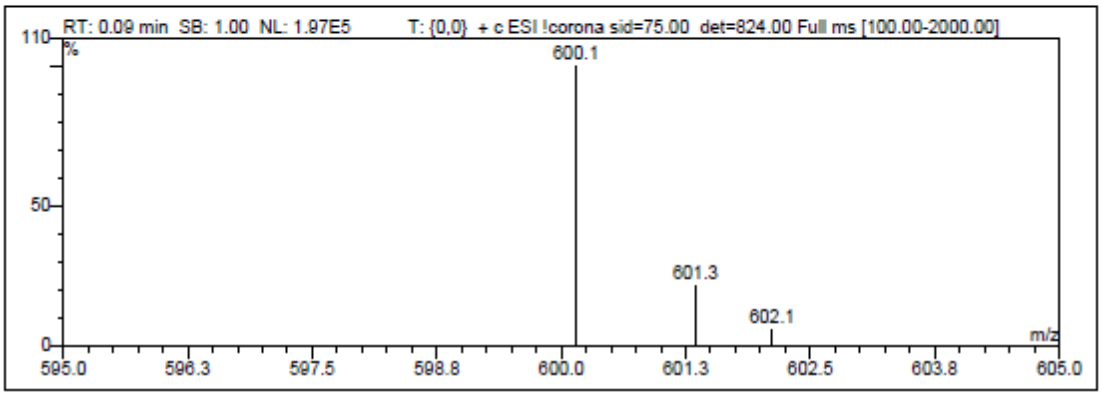

Figure S16. ESI-MS spectrum of **3**.

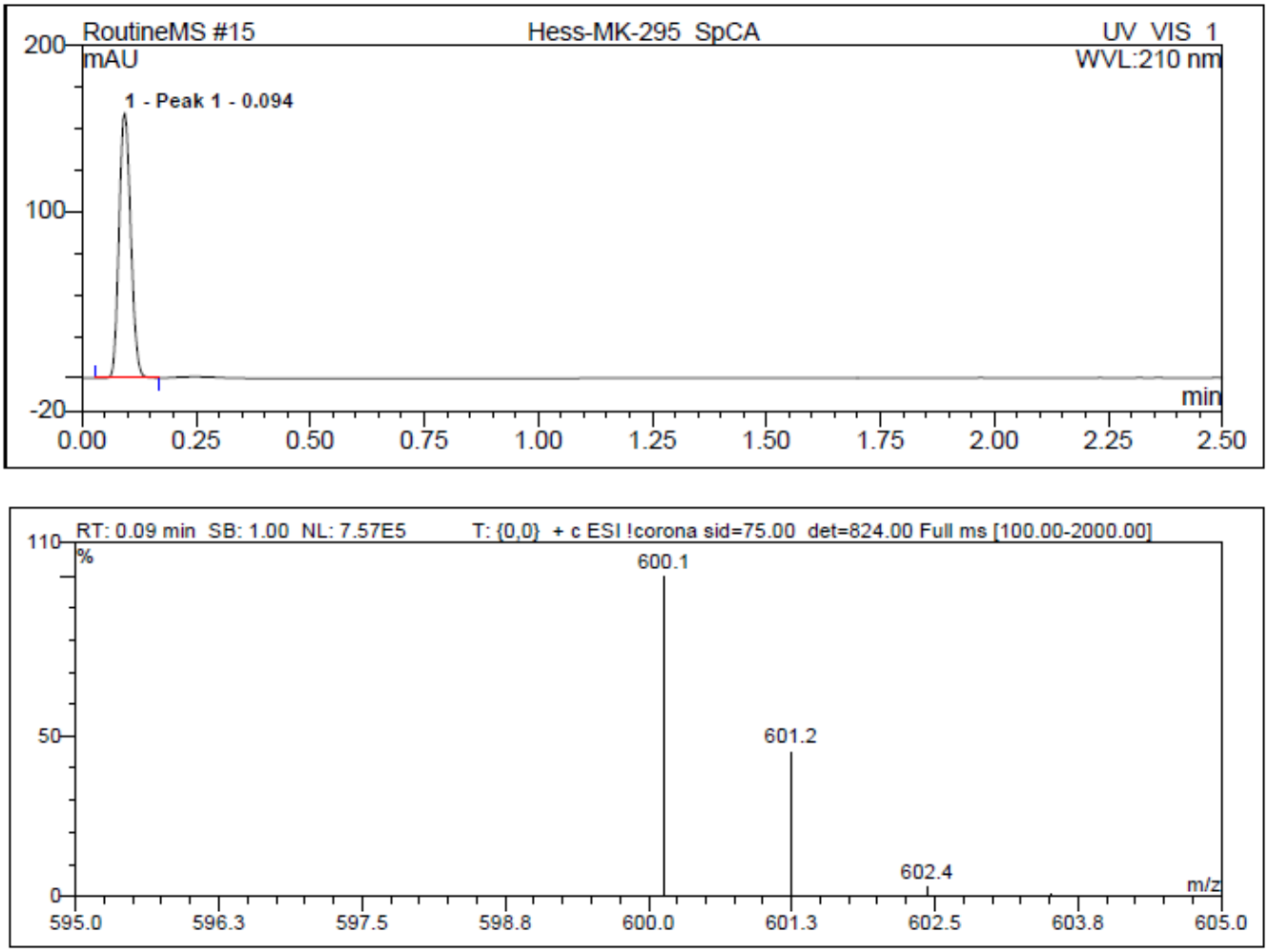

Figure S17. ESI-MS spectrum of a mixture of **3** and 5 equiv. *p*CA.

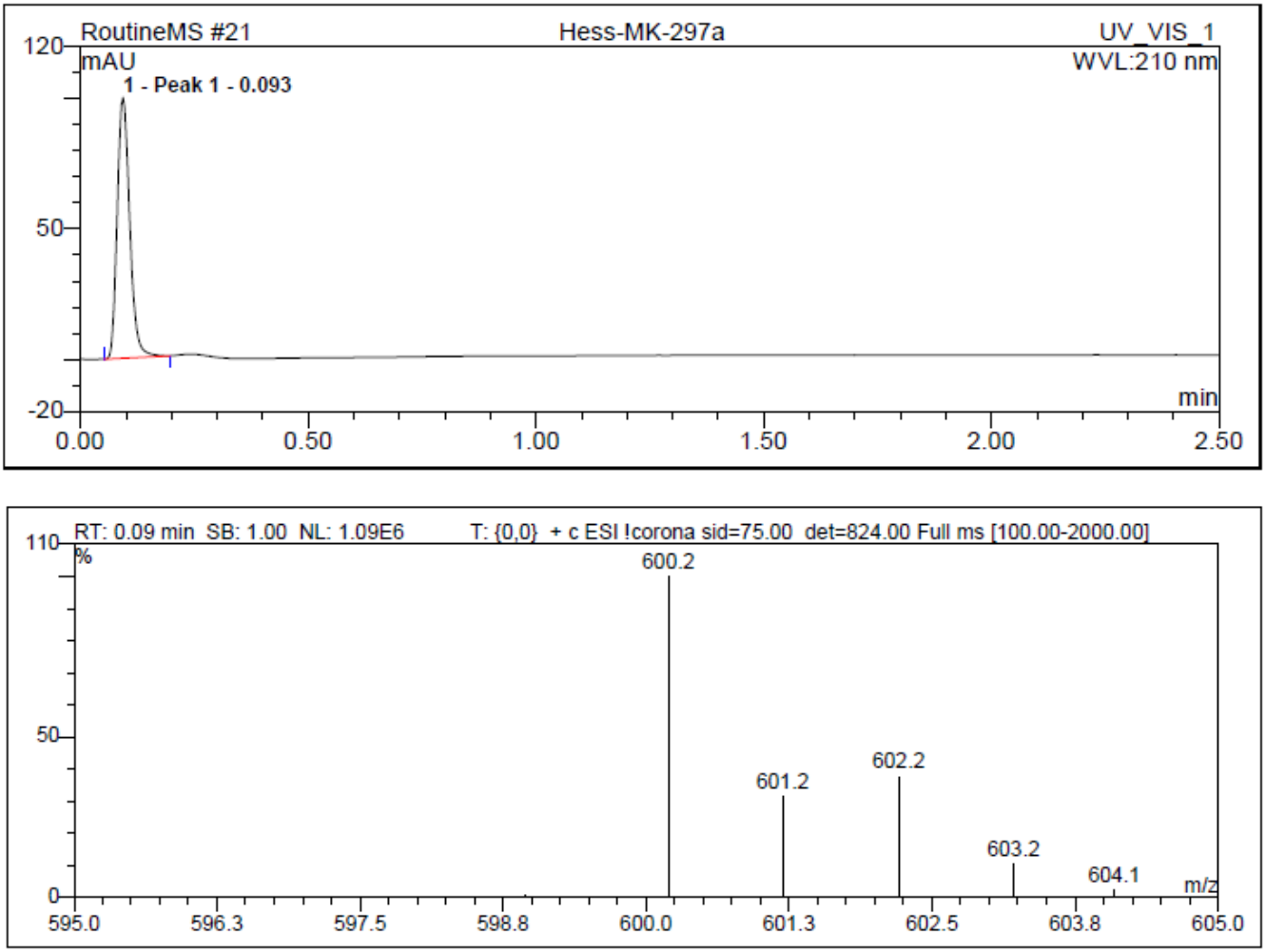

Figure S18. ESI-MS spectrum for the product of **1** plus 1 equiv. *p*CA.

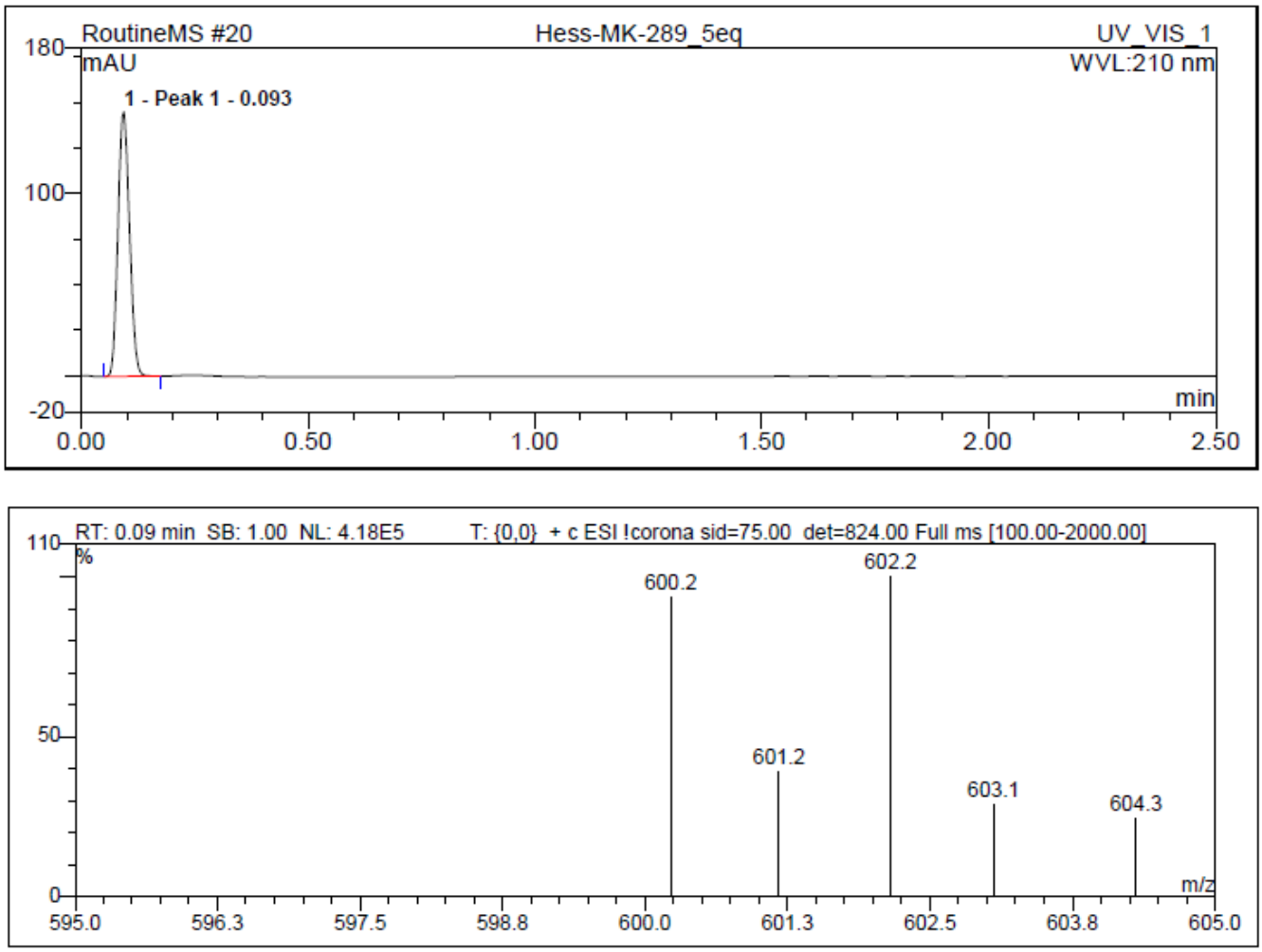

Figure S19. ESI-MS spectrum for the product of **1** plus 5 equiv. *p*CA.

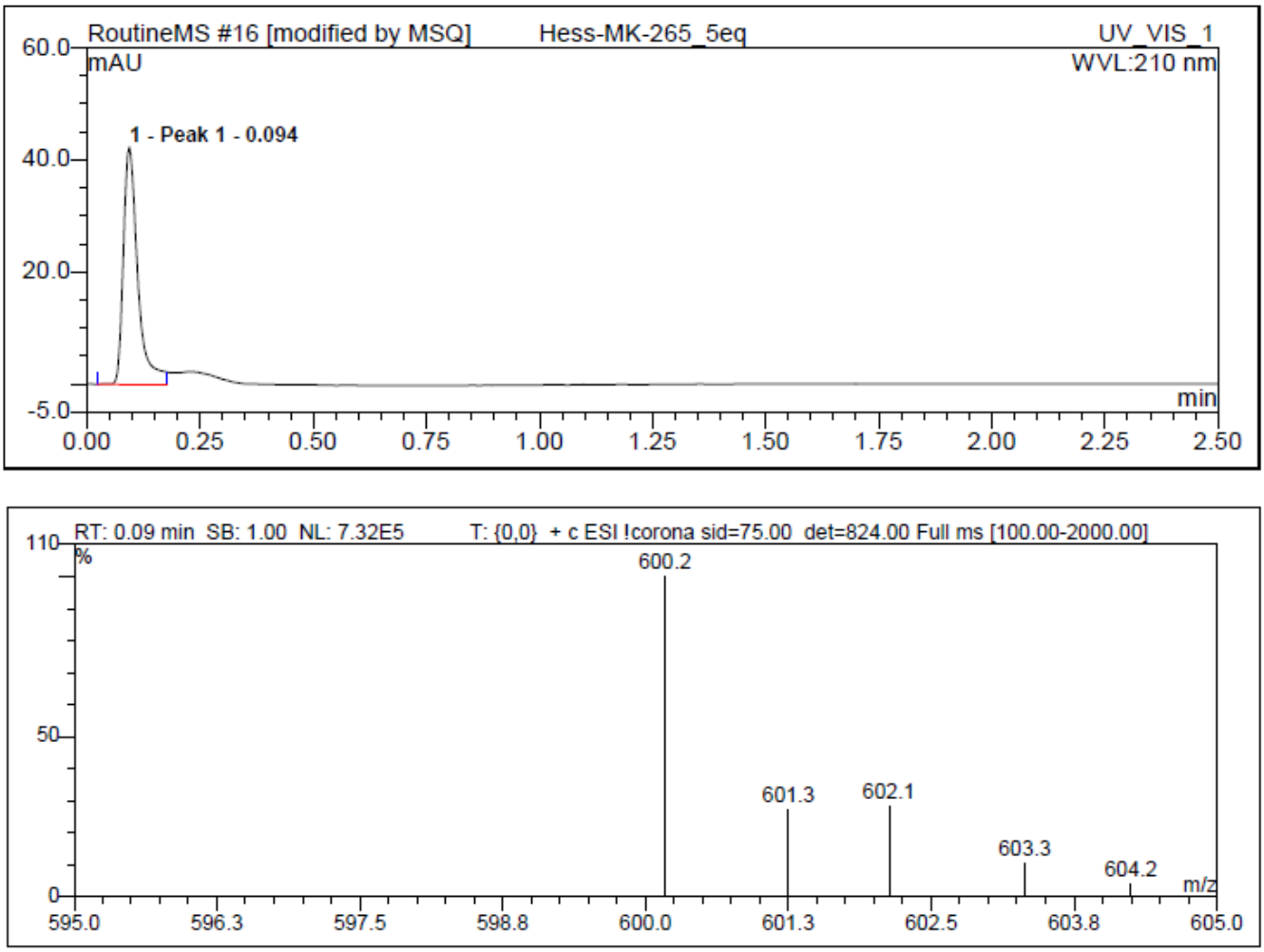

Figure S20. ESI-MS spectrum for the product of **1** plus 5 equiv. benzoic acid.

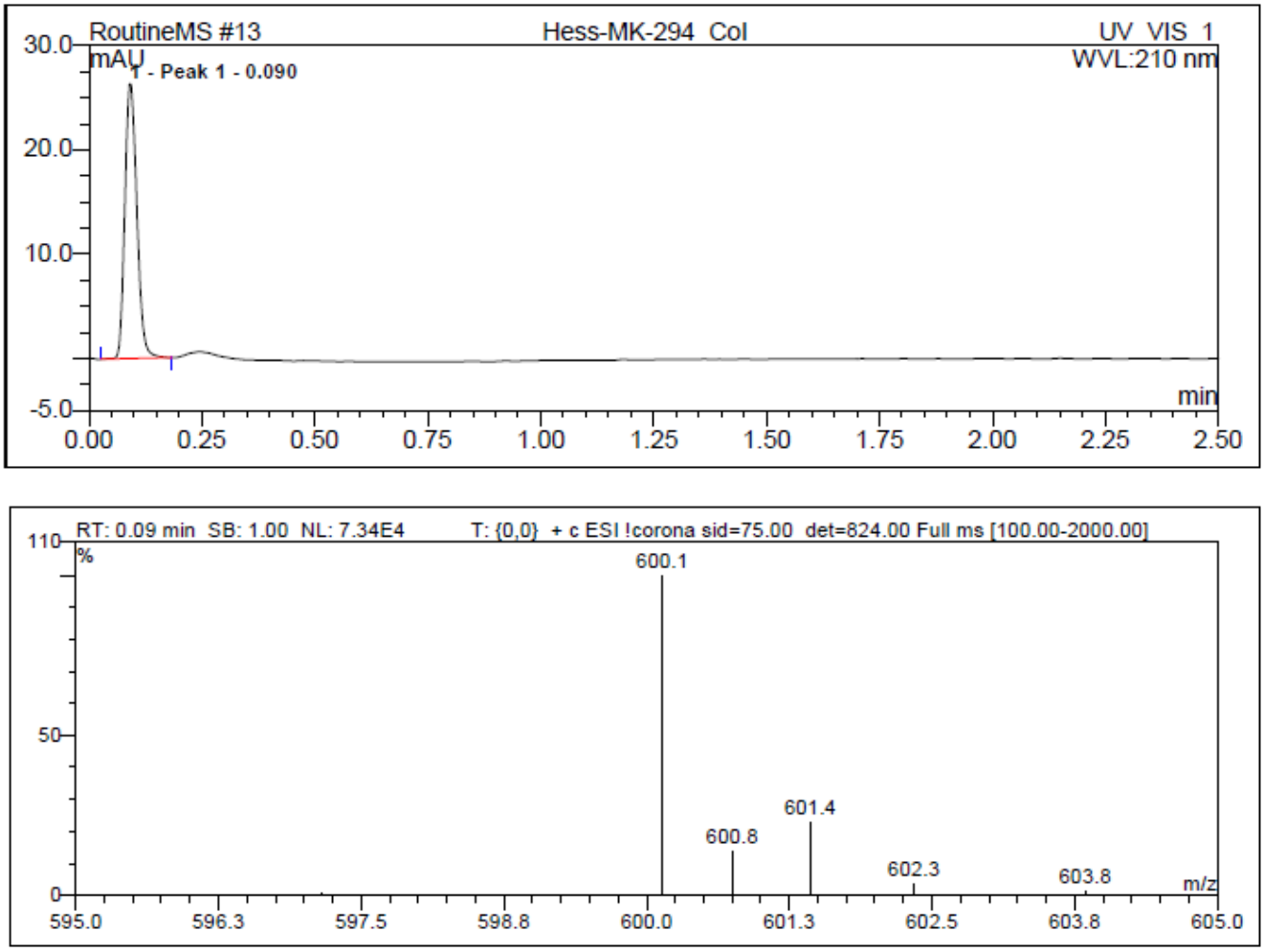

Figure S21. ESI-MS spectrum of **2**.

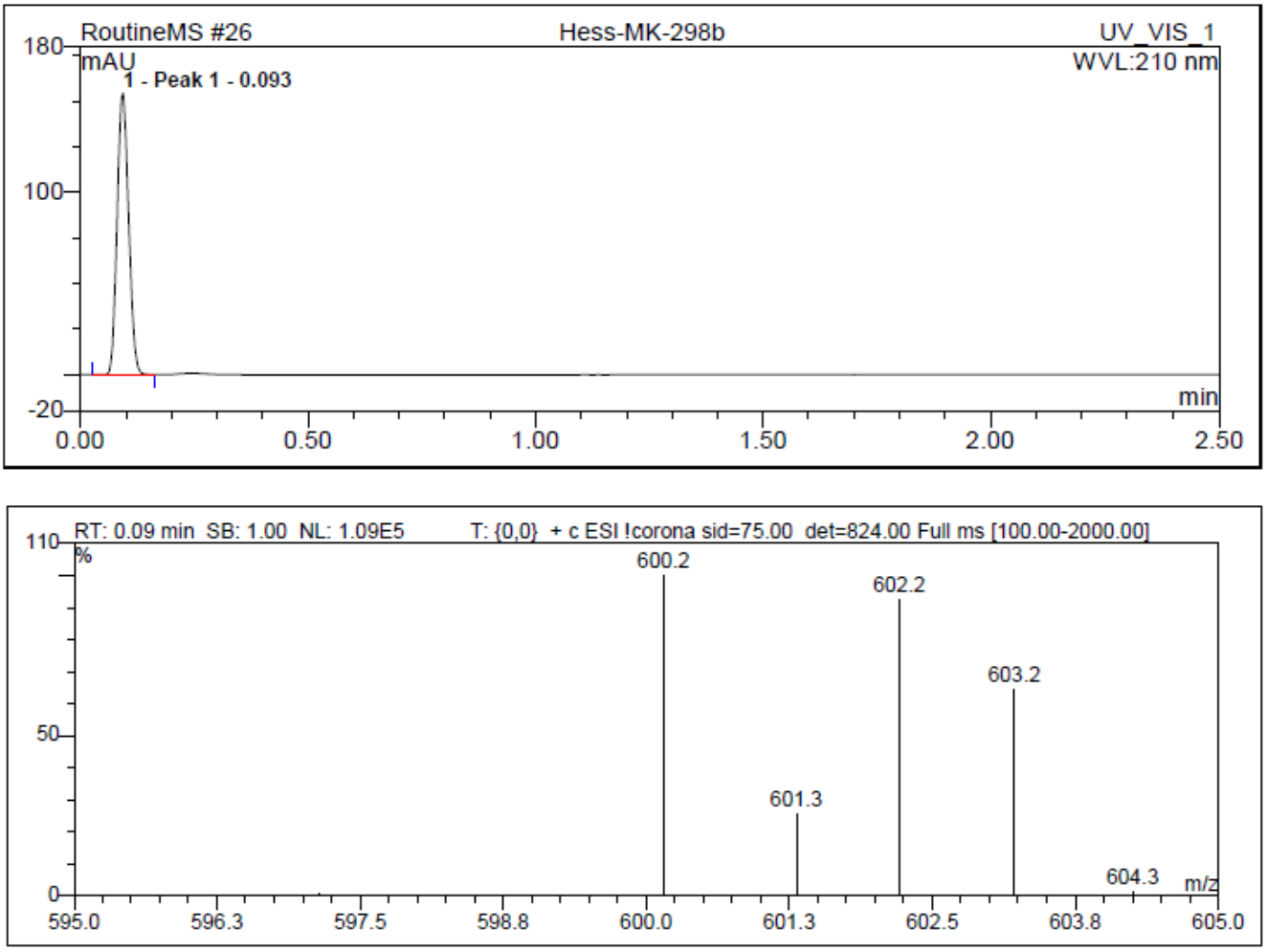

Figure S22. ESI-MS spectrum for the product of **2** plus 5 equiv. *p*CA.

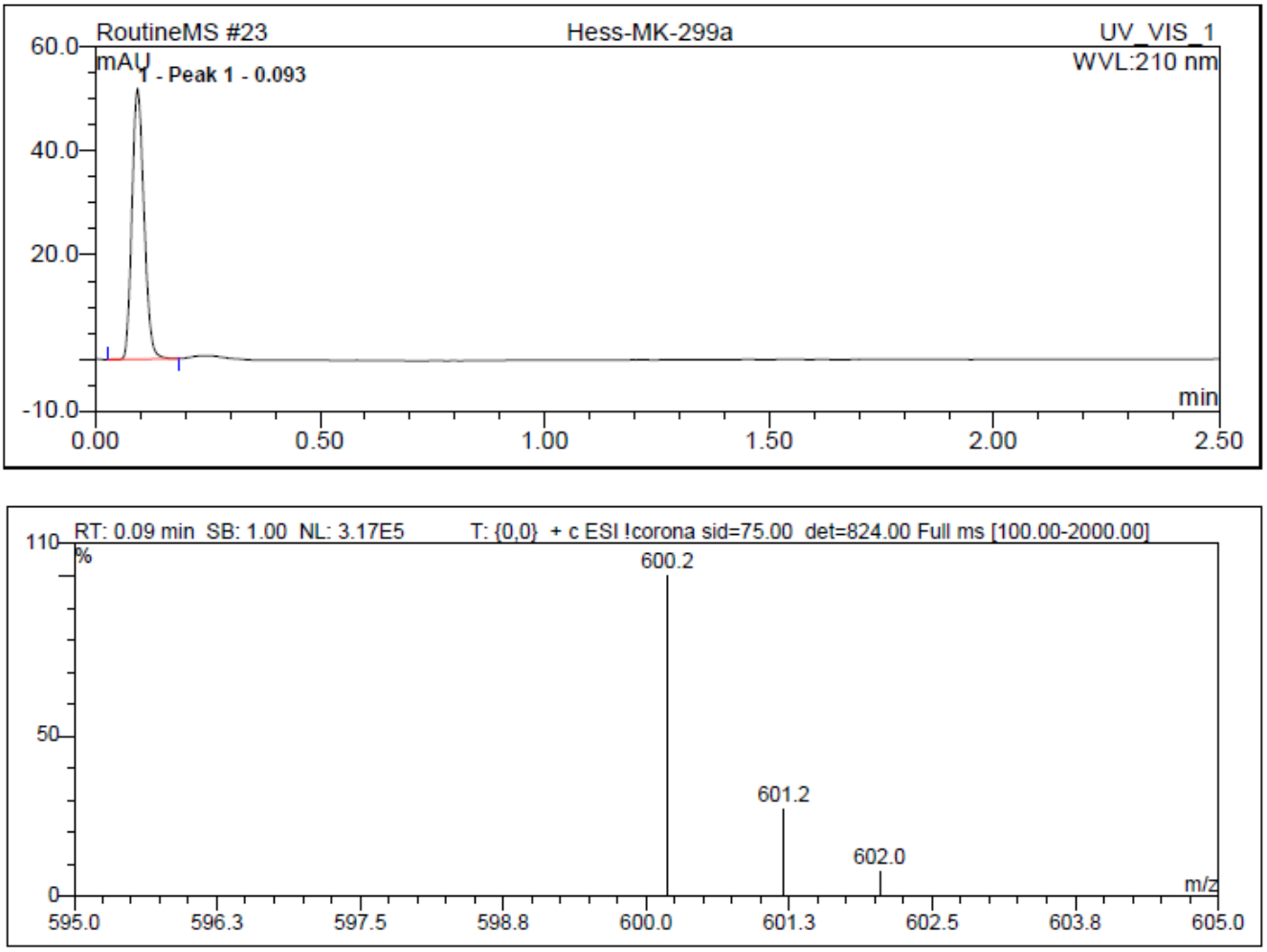

Figure S23. ESI-MS spectrum for the product of **2** plus 5 equiv. benzoic acid.

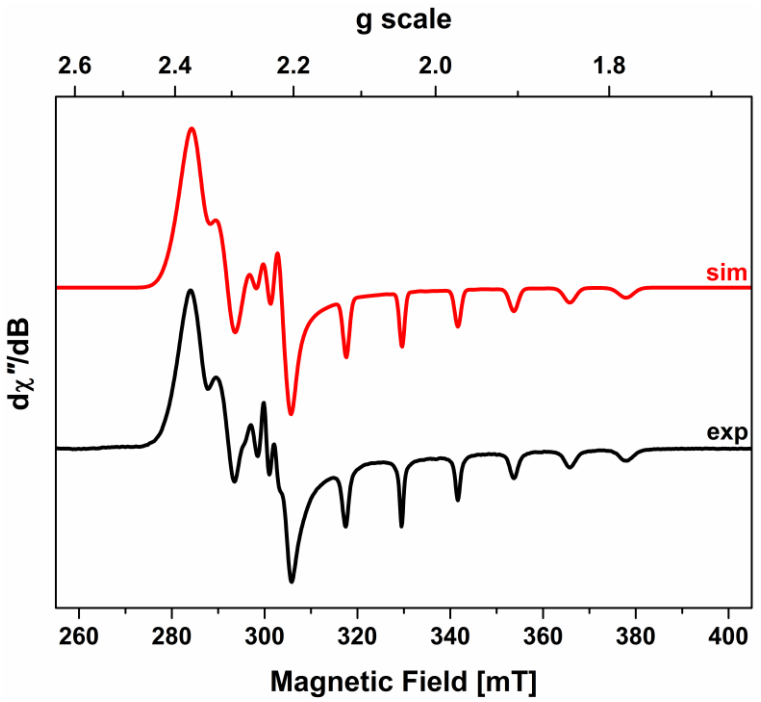

Figure S24. X-band EPR spectrum of **3** recorded in CH_2Cl_2/toluene solution at 130 K (experimental conditions: frequency, 9.4293 GHz; power, 0.63 mW; modulation, 0.3 mT). Experimental data are represented by the black line; simulation is depicted by the red trace: g = (2.285, 2.258, 2.006); $A\{^{59}Co\}$ = (26, 22, 113) × 10^{-4} cm^{-1}; Gaussian linewidths W = (10, 8, 6) × 10^{-4} cm^{-1}; g-strain σ_g = (-0.006, 0.006, 0.0007); A-strain σ_A = (-5, 1, -4).

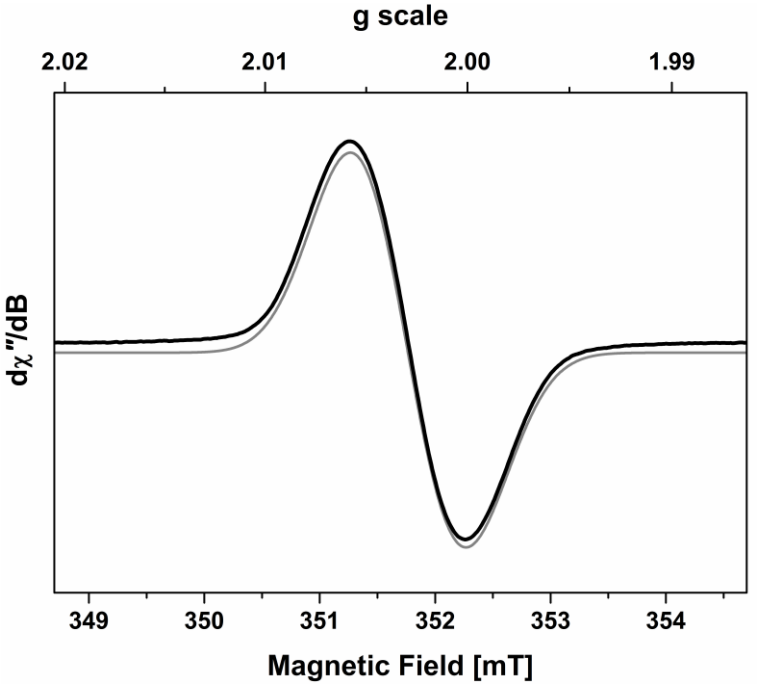

Figure S25. X-band EPR spectrum of **1** recorded in THF solution at 293 K (experimental conditions: frequency, frequency, 9.8612 GHz; power, 0.63 mW; modulation, 0.01 mT). Experimental data are represented by the black line and the simulation by the gray trace: g_{iso} = 2.0029; $A_{iso}\{^{59}Co\}$ = 1.05 × 10^{-4} cm^{-1}; Gaussian linewidth $W = 4.1 \times 10^{-4}$ cm^{-1}.

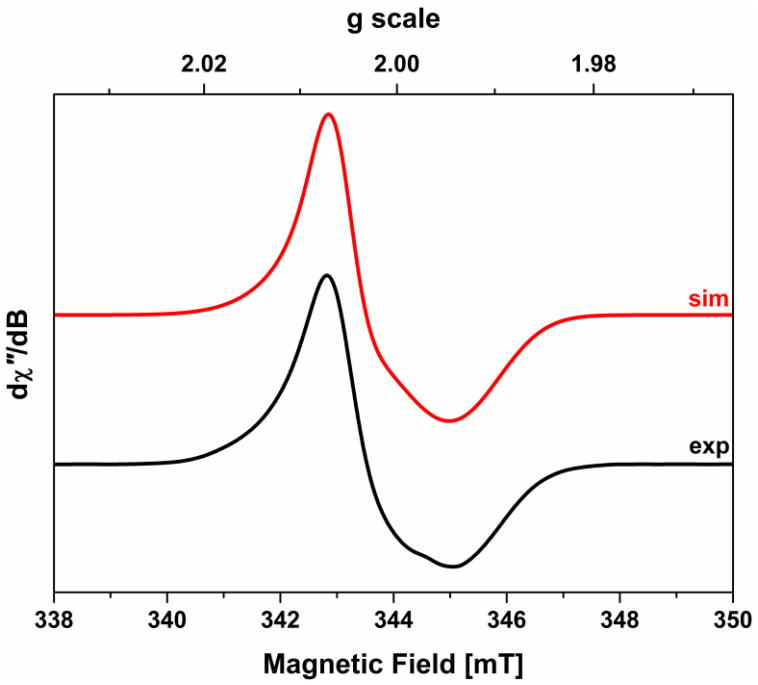

Figure S26. X-band EPR spectrum of **1** recorded in THF solution at 77 K (experimental conditions: frequency, frequency, 9.6311 GHz; power, 2.0 mW; modulation, 0.6 mT). Experimental data are represented by the black line; simulation is depicted by the red trace: g = (2.0056, 2.0042, 1.9941); $A\{^{59}\mathrm{Co}\}$ = (0, 1.5, 1.6) × 10^{-4} cm^{-1}; Gaussian linewidths W = (1.4, 13, 6.5) × 10^{-4} cm^{-1}; g-strain σ_g = (0.0009, 0, 0.0006).

SC-XRD determination of compound [2-H_2]

We performed a single-crystal XRD study on a crystalline specimen of **[2-H_2]**. Although the sample was of small size and limited quality, we were able to obtain a decent model of the structure. The refinement was possible until a stage, where we see strong indications of the addition of H-atoms. However, we were not able to proceed to the point, at which the crystal structure can be presented as a structural proof alone, but together with our results from the NMR experiments, the results from the diffraction experiments are presented as a supporting indication for the hydrogen addition to the ligand.

General crystal data

A dark violet plate-like specimen of $C_{33}H_{35}CoN_8$, approximate dimensions 0.008 mm x 0.115 mm x 0.220 mm, was used for the X-ray crystallographic analysis. The X-ray intensity data were measured on a Bruker D8 Venture system equipped with a Helios optic monochromator and a Mo TXS rotating anode (λ = 0.71073 Å).

The total exposure time was 20.15 hours. The frames were integrated with the Bruker SAINT software package using a narrow-frame algorithm. The integration of the data using an orthorhombic unit cell yielded a total of 82225 reflections to a maximum θ angle of 25.03° (0.84 Å resolution), of which 4932 were independent (average redundancy 16.672, completeness = 99.9%, Rint = 6.94%, Rsig = 2.63%) and 4123 (83.60%) were greater than 2σ(F2). The final cell constants of a = 9.993(2) Å, b = 20.714(5) Å, c = 27.024(6) Å, volume = 5594.(2) Å3, are based upon the refinement of the XYZ-centroids of 153 reflections above 20 σ(I) with 4.776° < 2θ < 41.17°. Data were corrected for absorption effects using the Multi-Scan method (SADABS). The ratio of minimum to maximum apparent transmission was 0.895.

The final anisotropic full-matrix least-squares refinement on F2 with 524 variables converged at R1 = 7.72%, for the observed data and wR2 = 15.18% for all data. The goodness-of-fit was 1.219. The largest peak in the final difference electron density synthesis was 0.466 e-/Å3 and the largest hole was -0.809 e-/Å3 with an RMS deviation of 0.075 e-/Å3. On the basis of the final model, the calculated density was 1.426 g/cm3 and F(000), 2512 e-.

Table S5. Sample and crystal data for **[2-H_2]**.

Identification code	KasMa27	
Chemical formula	$C_{33}H_{35}CoN_8$	
Formula weight	600.60 g/mol	
Temperature	100(2) K	
Wavelength	0.71073 Å	
Crystal size	0.008 x 0.115 x 0.220 mm	
Crystal habit	dark violet plate	
Crystal system	orthorhombic	
Space group	*P b c a*	
Unit cell dimensions	a = 9.993(2) Å	α = 90°
	b = 20.714(5) Å	β = 90°
	c = 27.024(6) Å	γ = 90°
Volume	5594.(2) $Å^3$	
Z	8	
Density (calculated)	1.426 g/cm^3	
Absorption coefficient	0.653 mm^{-1}	
F(000)	2512	
Diffractometer	Bruker D8 Venture	
Radiation source	TXS rotating anode, Mo	
Theta range for data collection	2.38 to 25.03°	
Index ranges	-11<=h<=11, -24<=k<=24, -32<=l<=32	
Reflections collected	82225	
Independent reflections	4932 [R(int) = 0.0694]	
Coverage of independent reflections	99.9%	
Absorption correction	Multi-Scan	
Refinement method	Full-matrix least-squares on F^2	
Refinement program	SHELXL-2014/7 (Sheldrick, 2014)	
Function minimized	$\Sigma w(F_o^2 - F_c^2)^2$	
Data / restraints / parameters	4932 / 188 / 524	
Goodness-of-fit on F^2	1.219	

Table S6. Data collection and structure refinement for **2-H_2**.

Δ/σ_{max}	0.001	
Final R indices	4123 data; I>2σ(I)	R1 = 0.0772, wR2 = 0.1457
	all data	R1 = 0.0930, wR2 = 0.1518
Weighting scheme	$w=1/[\sigma^2(F_o^2)+(0.0142P)^2+25.6150P]$ where $P=(F_o^2+2F_c^2)/3$	
Largest diff. peak and hole	0.466 and -0.809 eÅ^{-3}	
R.M.S. deviation from mean	0.075 eÅ^{-3}	

Refinement

First, we refined the structure using restraints (SAME, RIGU) for the split-layer positions of the aliphatic groups in the ligand backbone. The resulting intermediate model showed overall prolonged ADPs (Figure S31). Therefore, we also checked for lower symmetries and superstructure reflections, both not yielding improved results.

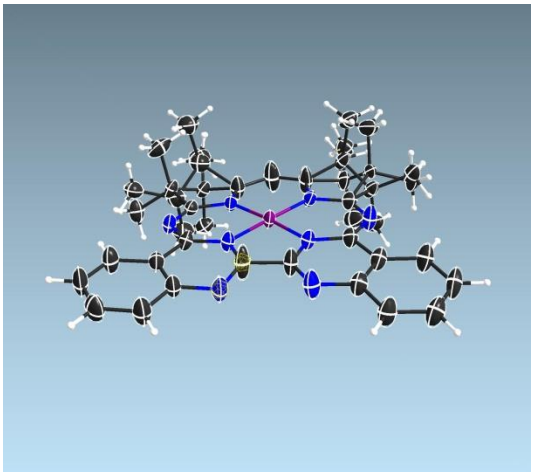

Figure S27. Refined structure of **[2-H_2]** showing prolonged ADPs especially at the bpm-moieties.

The ADPs for the distal nitrogen atoms in the bpm moiety and their adjacent central carbon atoms are significantly more elongated than their neighboring atoms. This is usually a sign for disorder, which is the first indication that the hybridization of these atoms could have be altered from sp^2 (compound **2**) to sp^3 after addition of hydrogen. The next indication for the presence of hydrogen atoms is the existence of positive peaks of residual electron density in close proximity of these elongated ADPs (Figure S32). The peaks are situated on opposite sides of the central complex plane and therefore could likely correspond to hydrogen atoms bound to the central carbon atom and the distal nitrogen atom, respectively.

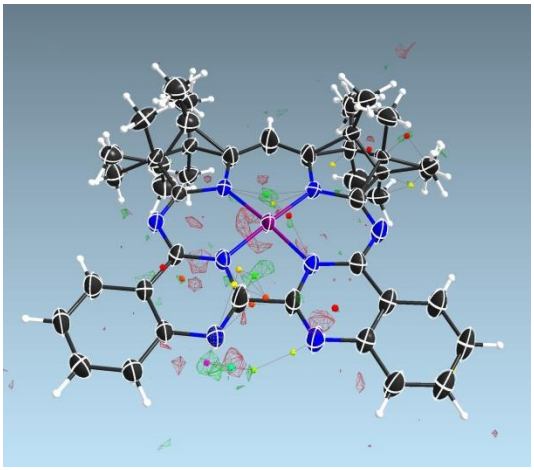

Figure S28. Refined structure of **[2-H$_2$]** showing two peaks in the positive residual electron density at the central atoms of the bpm-moieties. (The residual electron density at the metal atoms is caused by termination effects.)

A split-layer refinement was then performed, modelling a partial occupation of the sp^2-atoms (flat) or the sp^3-atoms, whereafter the two residual electron density peaks are in a meaningful distance to resemble N-H or C-H bonds respectively (Figure S33).

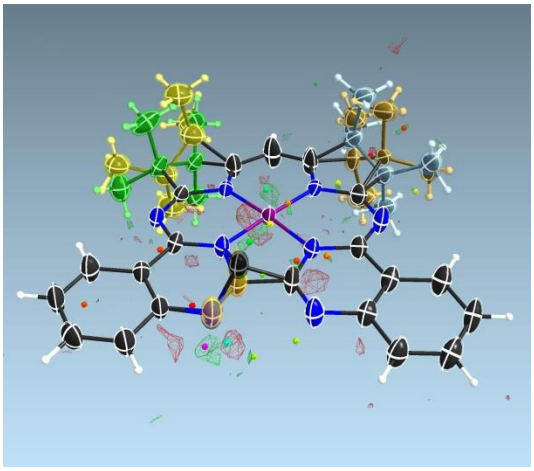

Figure S29. Refined structure of **[2-H$_2$]** showing the split-layer refinements with the two peaks in the positive residual electron density at the central atoms of the bpm-moieties. (The residual electron density at the metal atoms is caused by termination effects.)

This is the best model we were able to refine, since the addition of the protons at the peak positions does not enable the possibility to freely refine them (since their positions are refined towards the neighboring heavier atoms). We refrained from additional restraints to fix the H-positions and to model the same effect on the opposing side of the ligand, since the indications are already visible. Therefore, the SC-XRD determination strongly indicates, that the observed existence of additional H-atoms in the solution NMR-experiments can also be observed in the solid state.

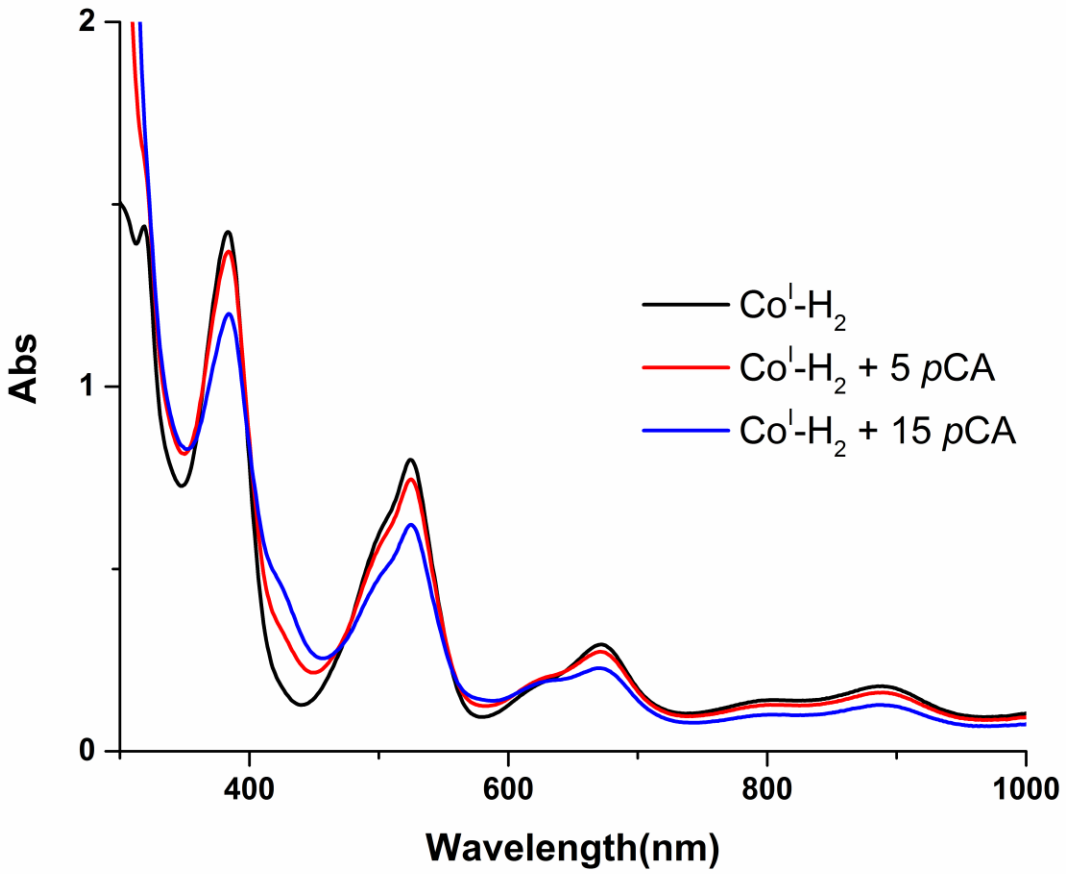

Figure S30. Electronic spectra of the reaction products of **[2-H$_2$]** with *p*CA.

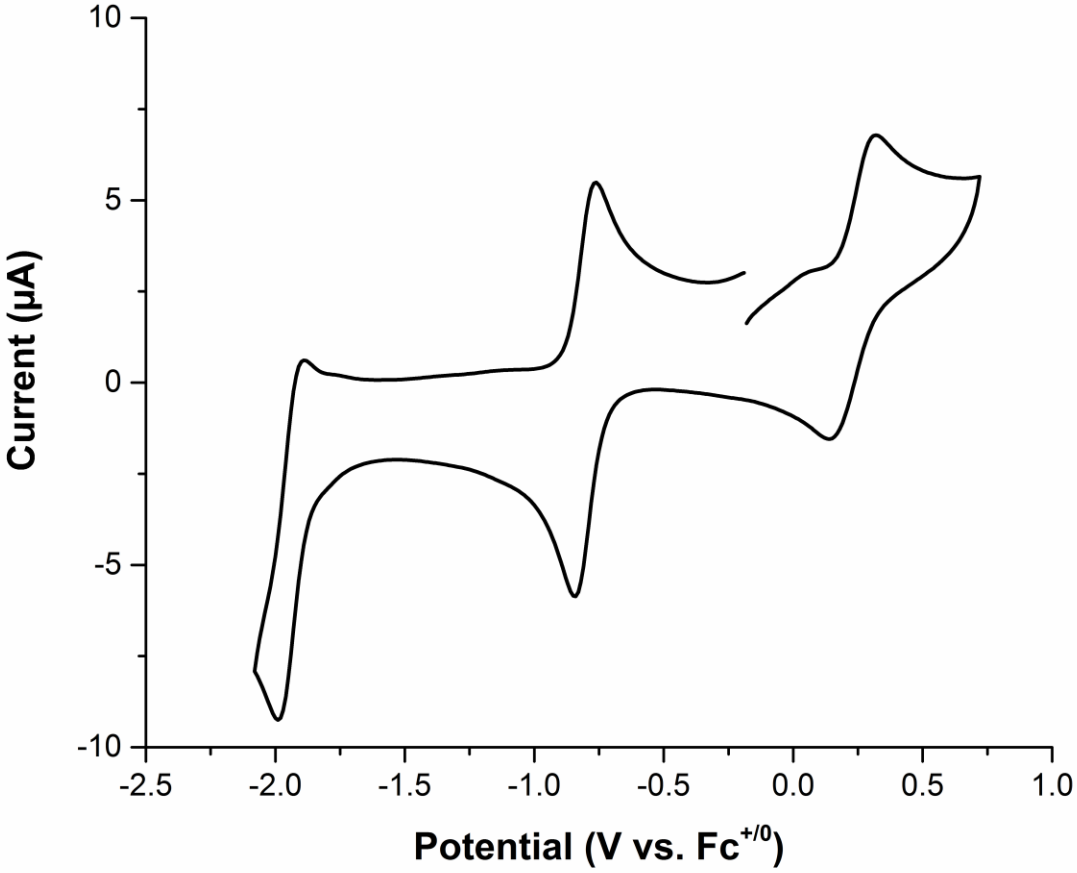

Fig. S31. Cyclic voltammogram of **[2-H_2]** (1.0 mM) in MeCN; 0.1 M [N(*n*-Bu)$_4$]PF_6; scan rate: 0.1 V/s.

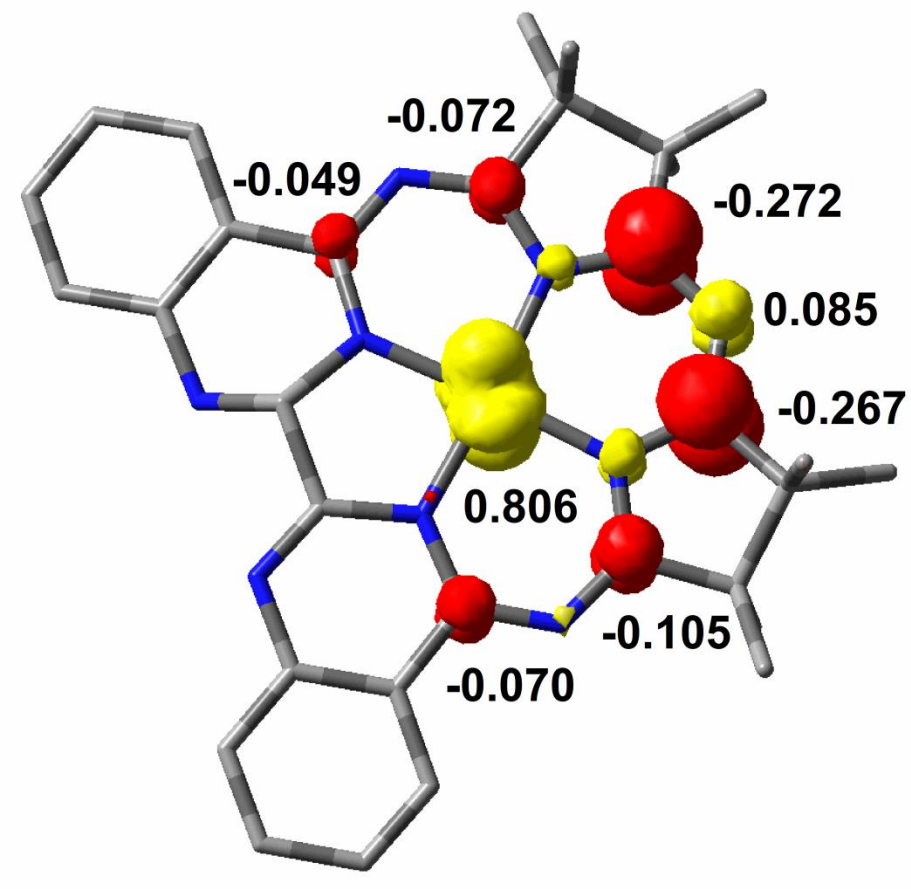

Fig. S32. DFT-derived (B3LYP) spin density plot for **[2-H_2]** based on Löwdin population analysis.

References

[1] D. Coucouvanis, *Useful Reagents and Ligands* in *Inorganic Syntheses, Vol. 33*, John Wiley & Sons, Inc., New York, **2002,** pp. 75-121.
[2] A. M. Appel, D. L. DuBois, M. Rakowski DuBois, *Journal of the American Chemical Society* **2005**, *127*, 12717.
[3] E. Müller, G. Bernardinelli, A. von Zelewsky, *Inorg. Chem.* **1988**, *27*, 4645.
[4] P. Banerjee, A. Company, T. Weyhermüller, E. Bill, C. R. Hess, *Inorg. Chem.* **2009**, *48*, 2944.
[5] E. V. Puttock, P. Banerjee, M. Kaspar, L. Drennen, D. S. Yufit, E. Bill, S. Sproules, C. R. Hess, *Inorganic Chemistry* **2015**, *54*, 5864.
[6] G. R. Hanson, K. E. Gates, C. J. Noble, M. Griffin, A. Mitchell, S. Benson, *J. Inorg. Biochem.* **2004**, *98*, 903.
[7] *APEX suite of crystallographic software, APEX 2, version 2008.4.*, Bruker AXS Inc.
[8] *SAINT, version 7.56a, SADABS, version 2008.1*, Bruker AXS Inc.
[9] C. B. Hübschle, G. M. Sheldrick, B. Dittrich, *SHELXLE, J. Appl. Crystallogr.* **2011**, *44*, 1281.
[10] G. M. Sheldrick, *SHELXL-2014*, University of Göttingen.
[11] G. M. Sheldrick, *SHELXL-97*, University of Göttingen.
[12] A. J. C. Wilson, *International Tables for Crystallography*, Dordrecht.
[13] A. L. Spek, *J. Appl. Cryst.* **2003**, *36*, 7.
[14] A. L. Spek, *Acta Cryst.* **2009**, *D65*, 148.
[15] A. L. Spek, *Acta Cryst.* **2015**, *C71*, 9.
[16] F. Neese, Version 3.0.3 ed., Max Plank Institute for Bioinorganic Chemistry, Mühlheim an der Ruhr, Germany, **Jan 2012**.
[17] A. D. Becke, *J. Chem. Phys.* **1986**, *84*, 4524.
[18] A. D. Becke, *J. Chem. Phys.* **1993**, *98*, 5648.
[19] C. T. Lee, W. T. Yang, R. G. Parr, *Phys. Rev. B* **1988**, *37*, 785.
[20] A. Schäfer, H. Horn, R. Ahlrichs, *J. Chem. Phys.* **1992**, *97*, 2571.
[21] A. Schäfer, C. Huber, R. Ahlrichs, *J. Chem. Phys.* **1994**, *100*, 5829.
[22] K. Eichkorn, O. Treutler, H. Ohm, M. Häser, R. Ahlrichs, *Chem. Phys. Lett.* **1995**, *240*, 283.
[23] K. Eichkorn, O. Treutler, H. Ohm, M. Häser, R. Ahlrichs, *Chem. Phys. Lett.* **1995**, *242*, 652.
[24] R. Dennington, T. Keith, J. Milliam, Version 5.0 ed., Semichem Inc., Shawnee Mission KS, **2009**.
[25] D. H. Pool, M. P. Stewart, M. O'Hagan, W. J. Shaw, J. A. S. Roberts, R. M. Bullock, D. L. DuBois, *Proc. Natl. Acad. Sci.* **2012**, *109*, 15634.